

# Identification of Potential *Candida albicans* Inhibitors Through Pharmacophore Modeling and Virtual Screening Techniques

## ABSTRACT

Fungal infections have increased significantly in recent years and represent a major threat to human health. A large number of these infections are caused by the opportunistic pathogen *Candida albicans*. Lanosterol 14- $\alpha$  demethylase (CYP51), a critical enzyme in the cytochrome P450 family, is a well-established target for antifungal drugs. However, the development of resistance to current antifungal treatments has created an urgent need to develop new inhibitors that are more effective and less likely to promote the emergence of resistance in *Candida albicans*. Azoles are a large and relatively new group of synthetic compounds, of which imidazoles and triazoles are two clinically useful families used in the treatment of systemic fungal infections.

In this study, we focused on *Candida albicans* and used the target protein (PDB code: 1EA1) to perform an in silico analysis of a series of benzimidazole derivatives. The aim was to identify novel chemotherapeutic agents with potential antifungal activity. To discover new *Candida albicans* inhibitors, pharmacophore models based on the molecular structure of benzimidazole derivatives were generated and validated using various methods. A virtual screening of the Enamine database containing 535,326 molecules was performed based on the combinatorial pharmacophore model. Compounds selected after virtual screening were subjected to molecular docking protocols (HTVS, SP, XP and IFD).

26 new compounds were identified and their absorption, distribution, metabolism and excretion (ADME) properties were calculated. These results suggest that the identified compounds could serve as promising chemical starting points for further structural optimisation in the development of *Candida albicans* inhibitors.

**Keywords** : Benzimidazole, *Candida albicans*, pharmacophore, virtual screening, molecular docking.

## 1. INTRODUCTION

Recently, fungal infections have significantly increased and have become serious threats to human health. Fungal infections can be classified into two types : superficial and systemic.[1].

Worldwide, fungal infections are responsible for more than 1.5 million deaths each year. They affect more than one billion people.[2]

The annual incidence of invasive fungal infections is approximately 6.5 million cases. The associated mortality is approximately 3.8 million.[3]

The increased incidence of candidiasis and the impressive rate of drug resistance have prompted researchers to develop new and more effective antifungal agents.

Opportunistic candidiasis, mainly *Candida albicans*, is responsible for this complicated fungal infection with 50 to 90% of human candidiasis [4, 5].

On the other hand, systemic infections are very dangerous, especially for immunocompromised people, including AIDS patients. [6, 7].

Many fungal infections such as neutropenia, endocarditis, endophthalmitis, meningitis, intra-abdominal candidiasis, osteomyelitis, and fungal arthritis are caused by the opportunistic pathogen *Candida albicans* [8]. Lanosterol 14- $\alpha$ -demethylase (CYP51), which belongs to the cytochrome P450 family, is a well-known and common antifungal target. [9, 10].

In clinical practice, there are limited antifungal agents that can be used for life-threatening fungal infections. These drugs fall into 5 main classes: azoles (Fluconazole, Itraconazole, Voriconazole, Ketoconazole), allylamines (Terbinafine, Naftifine), polyenes (Amphotericin B, Nystatine), fluoropyrimidines (Flucytosine) and thiocarbamates (Tolnaftate) [11].

Among them, azoles are the most widely used antifungal agents due to their high therapeutic index. Azoles are a large and relatively new group of synthetic compounds, of which imidazoles and triazoles are two clinically useful families used in the treatment of systemic fungal infections as well as in agriculture [12, 7, 13]. In this research, the combination of pharmacophore modelling, virtual screening and molecular docking was performed on a series of benzimidazole-derived molecules synthesised by Zon et al [14, 15] for the discovery of potential new inhibitors of *Candida albicans*.

## 2. Materials and methods

### 2.1 Selection of biological dataset

A data set of 74 benzimidazole derivatives with their antifungal activity MIQ (Minimum Inhibitory Quantity) ( $\mu\text{g}$ ) as inhibitors of fungal infection was obtained from the work of Zon et al. [14, 15]. All molecular structures and activity data utilized for pharmacophore modeling, virtual screening, and molecular docking are presented in Table 2. In these studies, the inhibitory activities MIQ (Minimum Inhibitory Quantity) values in M) for each compound were converted to their negative logarithmic form (pMIQ). All compounds share a similar structure and were evaluated using the same bioassay method.

### 2.2 Ligand preparation

The 3D structures of the ligands were generated using the construction panel in Maestro and optimized with the LigPrep module [16]. Partial atomic charges were assigned, and possible ionization states were generated at a pH of  $7.0 \pm 2.0$ . The OPLS\_2005 force field was employed to optimize the production of the lowest energy ligand conformer [17]. Energy minimization was performed for each ligand until it reached a root mean square deviation threshold of  $0.01 \text{ \AA}$ .

### 2.3 Pharmacophore model generation

Schrödinger's Phase module for ligand-based drug design was used to develop pharmacophore hypotheses [18]. The chemical characteristics of all ligands were defined by six pharmacophore features: hydrogen bond acceptor (A), hydrogen bond donor (D), hydrophobic group (H), negatively charged group (N), positively charged group (P), and aromatic ring (R). An active analogue approach was applied to identify common pharmacophore hypotheses, where common pharmacophores were selected from the conformations of the active ligand set using a hierarchical partitioning technique that groups similar pharmacophores based on their inter-site distances [19]. The identified pharmacophores were subsequently recorded and categorized. A scoring process was conducted to determine the most promising candidate hypothesis, which resulted in an overall ranking of all the hypotheses. The scoring algorithm took into account factors such as site point and vector alignment, volume overlap, selectivity, the number of paired ligands, relative conformational energy, and biological activity. [19].

### 2.4 Pharmacophore Validation

Validating a pharmacophore model is a crucial initial step to ensure its accuracy and specificity in selecting active molecules, while also guiding the virtual screening of ligands from a database. In this study, a set of 218 decoy molecules from the Directory of Useful Decoys (<http://dude.docking.org/>) [20],

21]supplemented with 20 active molecules, was used. These 20 *Candida albicans* inhibitors were not included in the construction of the pharmacophore models. Prior to validation, the preprocessing of both the active and decoy datasets was carried out using the LigPrep module. All possible ionizable states and tautomeric forms at a pH range of  $7.0 \pm 2.0$  were generated using this module[16]. For each compound, up to 32 conformers were generated by default, and low-energy stereoisomers with correct chirality were selected for further analysis. The Phase module's hypothesis validation tool[22]was employed for this process. This tool uses the hypothesis file along with the decoy and active datasets to calculate performance parameters. Several statistical parameters, including Enrichment Factors (EF), Robust Initial Improvement (RIE), Boltzmann Enhanced Discrimination of Receiver Operating Characteristic (BEDROC), Area Under the Accumulation Curve (AUC), and Receiver Operating Characteristics (ROC), were computed to validate the hypothesis[23].

## 2.5 Guner – Henry score validation

The Güner-Henry (GH) scoring method is employed to quantify the selectivity of a pharmacophore model and assess its effectiveness in similarity-based searching. This scoring method identifies the active molecules within a dataset comprising both known active and inactive compounds. The score ranges from 0 to 1, with 0 representing a null model and 1 indicating an ideal model. A score greater than 0.7 is typically expected[24].The formulas used to calculate the GH score are provided below:

$$GH = \left( \frac{H_a(3A + H_t)}{4H_t A} \right) \left( 1 - \frac{H_t - H_a}{D - A} \right)$$
$$\%A = \frac{H_a}{A} \times 100 ; \%Y = \frac{H_a}{H_t} \times 100 ; EF = \frac{H_a/H_t}{A/D}$$

In the GH scoring method,  $H_a$  represents the number of active compounds in the hits list (true positives),  $A$  is the total number of active compounds in the database,  $H_t$  is the total number of hits retrieved, and  $D$  is the total number of compounds in the database.  $\%A$  indicates the percentage of known active compounds obtained from the database, while  $\%Y$  refers to the percentage of known active compounds in the hits list. EF stands for the enrichment factor, which quantifies the concentration of actives retrieved by the model compared to random screening without using a pharmacophore approach. The Güner-Henry score is considered an important metric, as it accounts for both the percentage yield of actives in the database ( $\%Y$ ) and the percentage ratio of actives in the hits list ( $\%A$ ).

## 2.6 High throughput virtual screening and molecular docking

The molecules obtained after pharmacophore screening were subjected to filtering through High Throughput Virtual Screening (HTVS)[25], followed by Glide docking using Standard Precision (SP) and Extra Precision (XP)[26]methods at the crystal structure binding sites with Glide. The co-crystallized ligand was centered for grid generation using Glide's grid generation tools. Post-docking minimization was carried out using MM-GBSA (Molecular Mechanics energies combined with Generalized Born and Surface Area)[27] to optimize the geometries of the retrieved molecules. The top 10% of the molecules from each step were selected for further analysis. Finally, all non-peptide molecules (since peptide compounds are orally degradable) were processed using the Glide XP molecular docking system, employing the 1EA1 crystal structure to evaluate the docking scores of the resulting molecules after screening. The selection of the 1AE1 target protein, which represents the CYP51 enzyme of *Mycobacterium tuberculosis* (MTCYP51), is based on several factors. MTCYP51 provides a structurally resolved and well-characterised model system for studying inhibition of the enzyme by antifungal agents such as fluconazole and itraconazole[28]. The crystal structures of MTCYP51 bound to antifungal agents provide essential information on the catalytic mechanism of the enzyme, the architecture of its active site and its interactions with ligands[29]. In addition, its similarity to fungal CYP51 in terms of drug-binding characteristics and functional motifs makes it a relevant surrogate for the study of antifungal resistance mechanisms.

## 2.7 Induced fit docking

An induced fit docking (IFD) method[30, 31], where the receptor is flexible during the docking process, was employed in this study. The energy minimization of the protein structure was carried out using the OPLS\_2005 force field. The prepared molecules were docked to the rigid protein using Glide with default parameters. Energy minimization was applied to the crystal structure of PDB code: 1EA1. XP

molecular docking was used for the initial docking, and 25 ligand poses were retained for the refinement of the protein structure. Schrödinger's 2017-4 Prime module was then used to refine residues within 5.0 Å of the ligand poses, leading to the development of induced fit protein-ligand complexes. After these refinements[32], the ranking of each of the 26 complexes was performed based on Prime energy. Complexes with an energy below -25 kcal/mol were re-docked for the final step of scoring. Each ligand was docked into the refined low-energy receptor structures developed during the refinement step. The binding affinity of each complex was estimated using the docking score. The lowest negative docking and IFD scores were considered to represent the most favorable binding conditions with the active site of 1EA1.

## 2.8 ADME prediction

The QikProp tool from Schrödinger[33] was used to predict the drug-like properties of the ten best hits by evaluating their ADME (Absorption, Distribution, Metabolism, and Excretion) profile. During this process, the Lipinski rule of five was applied, and various descriptors, such as QPPCaco, QPlogBB, and the percentage of human oral absorption, were calculated.

## 3. Results and discussions

### 3.1 Generation of pharmacophore models

We developed ligand-based pharmacophore models that identified the pharmacophore points required to inhibit the biological activity of *Candida albicans*. The molecules in the dataset were divided into active, inactive and moderately active molecules. Molecules with a pMIQ ( $pMIQ = -\log(MIQ)$ ) greater than 8 were considered active and those with a pMIQ less than 7.5 were considered inactive, while compounds with a pMIQ between the threshold values were considered moderately active.

Pharmacophore models containing 4 to 5 sites were generated using four features: hydrogen bond acceptor (A), hydrogen bond donor (D), hydrophobic (H) and aromatic ring (R). The quality of the pharmacophore models was evaluated using site score, vector score, volume score, survival score and BEDROC score[34]. Among the generated pharmacophore models, the eight best models (Table 1) were selected on the basis of the survival score parameter. A good pharmacophoric model is characterised by a high value of the parameters Survival score[34]. The models obtained have a survival score between 4.483 and 5.324. (Table 1) The ADRRR\_1 model has the highest survival score of 5.324. This model includes a hydrogen bond acceptor (A), a hydrogen bond donor (D) and three aromatic rings (R).

### 3.2 Validation of the pharmacophore : the Decoy method

The constructed pharmacophore models were validated using a set of parameters (Table 3) calculated from a database containing 218 decoy molecules, enriched with 20 *Candida albicans* inhibitors that were not used in the construction of the pharmacophore models. The database was screened with the pharmacophores obtained using the phase software screening tool. For the different pharmacophoric models, the enrichment factor at 1% is between 5.95- 11.90 and the GH (goodness of hit) parameter is between 0.78 and 1. These results indicate that the different pharmacophores generated show a high selectivity with respect to the active molecules.

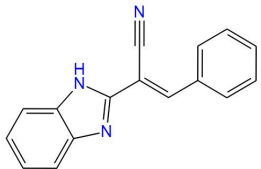
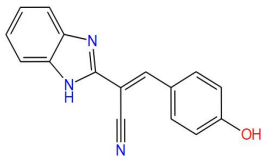
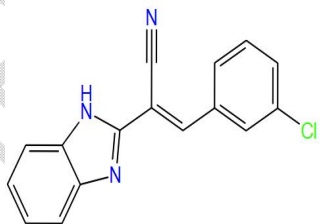
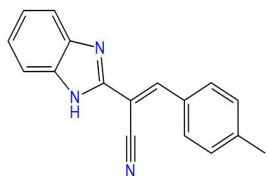
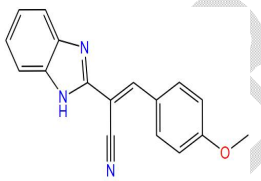
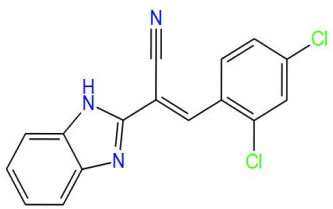
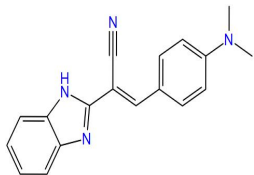
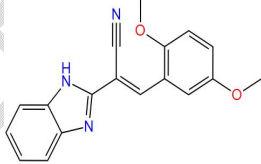
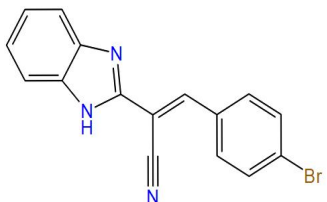
**Table 1.the obtained pharmacophore models and Scoring parameters**

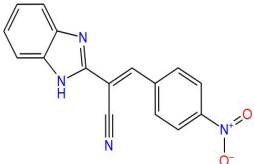
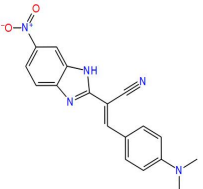
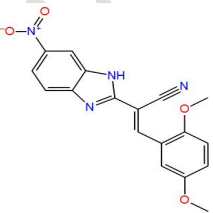
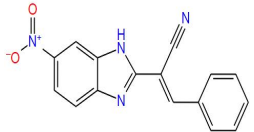
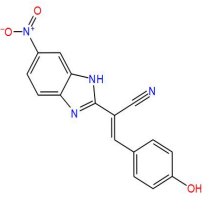
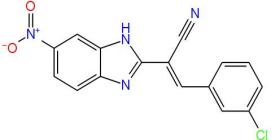
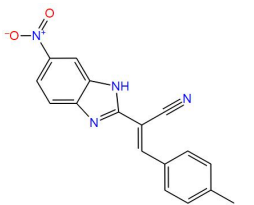
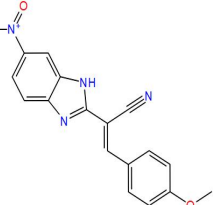
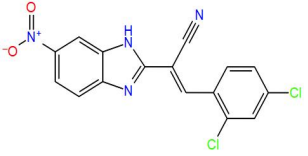
Model	Vector Score	Volume Score	Survival Score	Site Score	Selectivity Score	Adjusted Score	BEDROC Score	PHS <sup>a</sup>
ARRR_1	0.938	0.760	5.224	0.817	1.277	5.224	0.754	1.068
ARRR_2	0.881	0.619	4.895	0.586	1.265	4.895	0.523	0.817
HRRR_1	0.784	0.579	4.953	0.502	1.531	4.953	0.465	0.763
ADRR_1	0.923	0.726	5.198	0.804	1.201	5.198	0.716	1.028
ADRR_2	0.991	0.872	4.883	0.918	1.199	4.883	0.520	0.813
ADRRR_2	0.982	0.872	5.285	0.900	1.627	5.285	0.535	0.852
ADRRR_1	0.982	0.873	5.324	0.899	1.668	5.324	0.526	0.846
AADRR_2	0.982	0.873	5.076	0.892	1.426	5.076	0.533	0.838

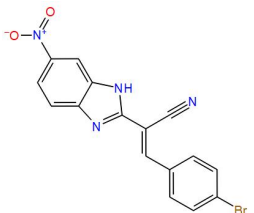
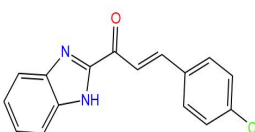
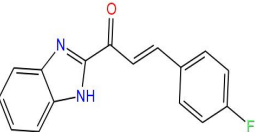
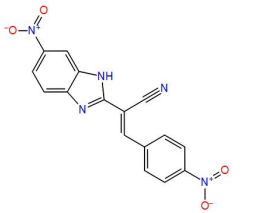
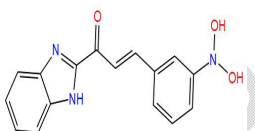
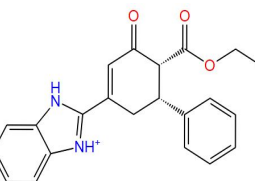
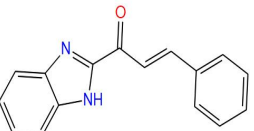
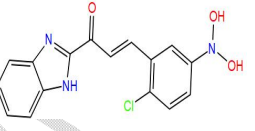
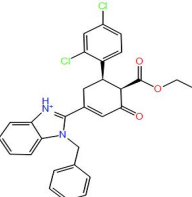
a :Phase hypo score

UNDER PEER REVIEW

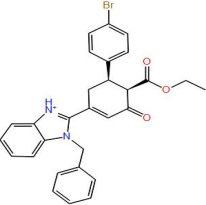
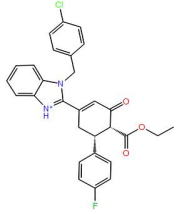
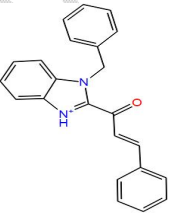
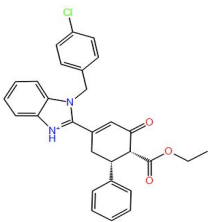
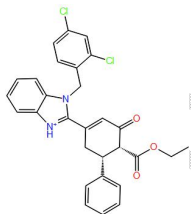
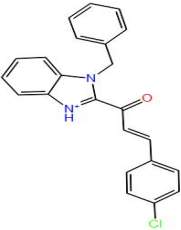
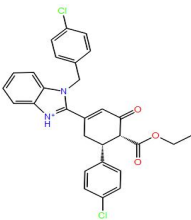
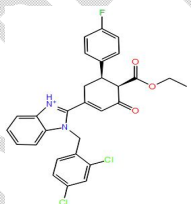
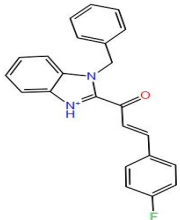
**Table2. Structure of benzimidazoles and their biological activities pMIQ**

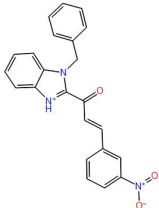
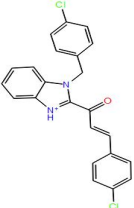
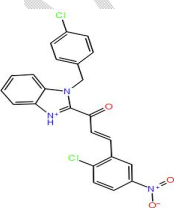
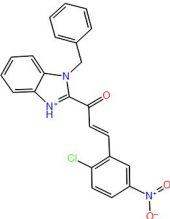
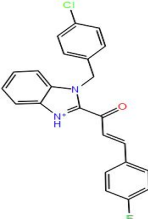
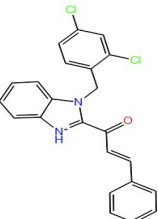

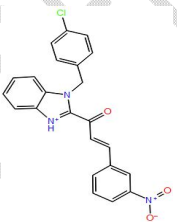
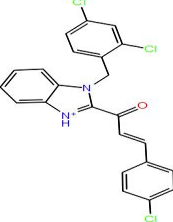
Ligands	Structure	Activity	Ligands	Structure	Activity	Ligands	Structure	Activity
A1		7.3897	A4		7.4171	A7		7.4467
A2		7.4138	A5		7.439	A8		7.4972
A3		7.4599	A6		7.485	A9		7.5108

Ligands	Structure	Activity	Ligands	Structure	Activity	Ligands	Structure	Activity
A10		7.462 8	A13		7.523	A16		7.5445
A11		7.462 8	A14		7.486	A17		8.4146
A12		7.483 3	A15		7.505	A18		9.3512

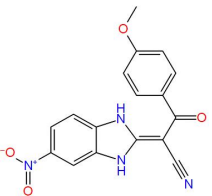
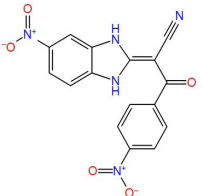
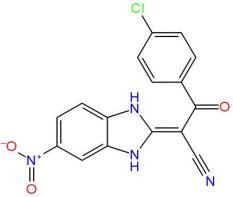
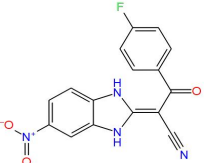
Ligands	Structure	Activity	Ligands	Structure	Activity	Ligands	Structure	Activity
A19		9.363 1	A22		7.451	A25		8.6295
A20		7.525 4	A23		7.467	B26		7.5568
A21		8.298 0	A24		7.515	B27		7.7155



Ligands	Structure	Activity	Ligands	Structure	Activity	Ligands	Structure	Activity
B28		7.723 8	B31		7.701 5	B34		7.5294
B29		7.685 7	B32		7.715 5	B35		7.5715
B30		7.715 5	B33		7.730 3	B36		7.5519

Ligands	Structure	Activity	Ligands	Structure	Activity	Ligands	Structure	Activity
B37		7.583 7	B40		7.609 9	B43		7.9564
B38		7.621 0	B41		7.592 0	B44		7.6099
B39		7.571 5	B42		7.621 0	B45		7.6452

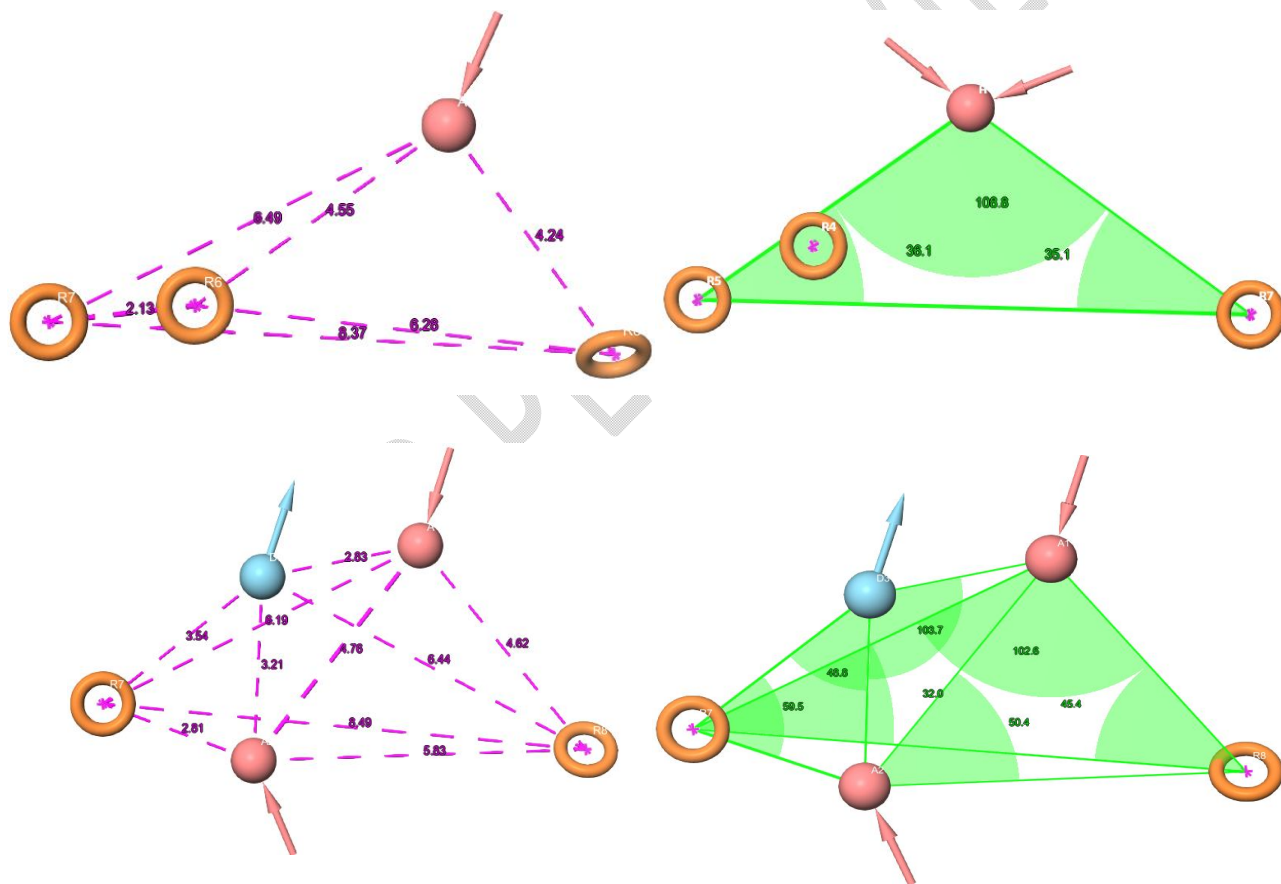
Ligands	Structure	Activity	Ligands	Structure	Activity	Ligands	Structure	Activity
B46		7.628 7	C49		7.417 1	C52		7.4460
B47		7.655 4	C50		7.464 4	C53		7.4861
B48		7.687 3	C51		7.470 9	C54		7.4861

Ligands	Structure	Activity	Ligands	Structure	Activity	Ligands	Structure	Activity
C55		7.526 7	C58		8.750 1			
C56		7.532 4						
C57		7.510 9						

**Table3. Validation of pharmacophore models by the DECOY method**

Model	D	A	Ht	Ha	%Y	%A	FN	FP	EF1	BEDROC	ROC	AUC	RIE	GH
ARRR_1	238	20	27	20	74.07	100	0	7	11.90	1.00	0.97	0.93	8.49	0.7797
ARRR_2	238	20	25	20	80	100	0	5	11.90	1.00	0.98	0.94	8.56	0.8305
HRRR_1	238	20	27	20	74.074	100	0	7	5.95	0.75	0.97	0.93	7.11	0.7797
ADRR_1	238	20	21	20	95.24	100	0	1	11.90	1.00	1.00	0.95	9.38	0.9599
ADRR_2	238	20	21	20	95.24	100	0	1	11.90	1.00	0.99	0.95	9.30	0.9599
AADRRR_1	238	20	21	20	95.2381	100	0	1	11.90	1.00	1.00	0.95	9.38	0.9599
AADRR_2	238	20	21	20	95.2381	100	0	1	11.90	1.00	0.99	0.95	9.30	0.9599
ADRR_2	238	20	20	20	100	100	0	0	11.90	1.00	0.50	0.73	6.76	1.0000

a) ARRR\_1

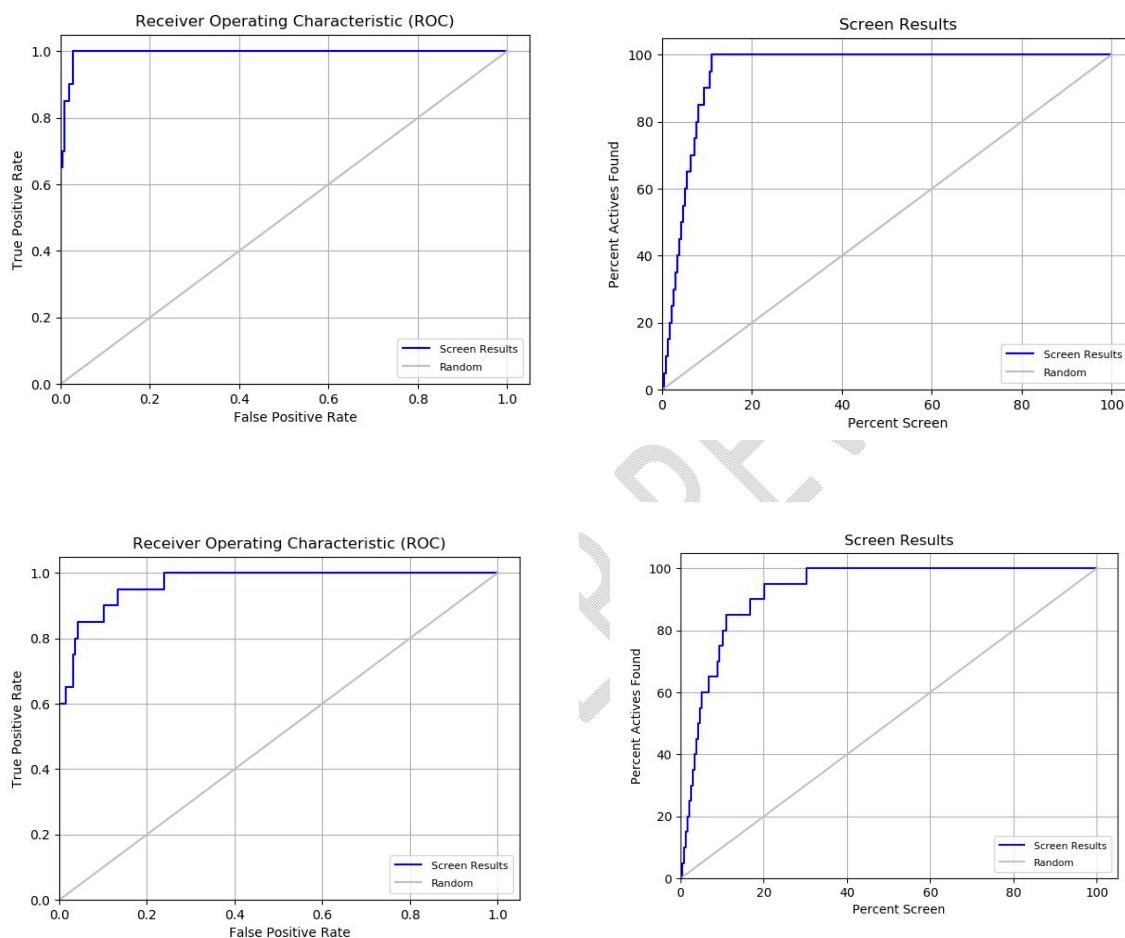


b) AADRR\_2

**Fig. 1. 3D representation of the pharmacophore models a) ARRR\_1 b) AADRR\_2 with distances and angles between the different pharmacophore sites.**

These results indicate that the different pharmacophores generated show a high selectivity towards the active molecules. The different hits obtained during the validation were also statistically analysed using the ROC curve, which is a graphical representation of the relationship between the sensitivity and specificity of the virtual screening process. The ROC curve represents the fraction of VPs (among the active) versus the VNs (among the inactive) obtained during the screening of the database. The

parameter characterising the ROC curve is between 0 and 1. Truchon and Baylay [35] considered an ROC value of 0.7 as a desirable performance value. In the present study, the ROC parameters of the different pharmacophore models ranging from 0.97 to 1 indicate that the different models are able to distinguish active from inactive molecules in the virtual screening process (Fig.2).



**Fig. 2.ROC curve of the pharmacophore models AADRR\_2 , ARRR\_1**

The AUC metric of the ROC curve was also considered to test the performance of the different pharmacophorical models. The pharmacophore models obtained have a significant AUC between 0.73-0.95 (Table 3). These values of the AUC metric highlight the reliability of the different pharmacophore models in identifying new compounds in a virtual screening experiment. Consequently, all the parameters calculated for the assessment of the quality of the pharmacophores suggest that these pharmacophoric models have a high predictive power in the identification of active compounds in a chemical library thus providing a starting point for the identification of new inhibitors of *candida albicans*.

### 3.3 Virtual screening of the Enamine chemical library

Virtual screening based on ligands from a database of molecules (chemical library) is a widely used technique in the drug design process for the identification of new hits [36]. Screening a database using pharmacophore models facilitates the screening of millions of multi-conformational compounds at once. The validated pharmacophore models were used for virtual screening of the phase.dtb database created from the "sdf" format files from the ENAMINE database. This database contains 535326, Molecules approximately 13383150 conformations. The screening of the database using

pharmacophore models as "three-dimensional queries" yielded 78,000 molecules which were then used in the VSW (Virtual Screening Workflow) protocol of the Schrodinger suite. The VSW protocol is a multi-step virtual docking screening process of the Schrodinger package, which includes different steps with increasing molecular docking accuracies. This protocol was used to screen by molecular docking the compounds obtained after screening the database by the different pharmacophore models.

**Table 4. Hits obtained after virtual screening using pharmacophore models and molecular docking**

Title	Vector Score	Matched Ligand Sites	Hypo ID	Align Score	Phase Screen Score	Fitness	Volume Score
Z1804044680	0.837	A(1) R(11) R(10) R(12)	ARRR_1	0.452	2.025	2.025	0.564
PV-001850708261	0.842	A(4) R(11) R(10) R(12)	ARRR_2	0.440	2.094	2.094	0.618
Z2283404606	0.916	H(7) R(9) R(8) R(10)	HRRR_1	0.381	2.041	2.041	0.442
Z1651668373	0.816	H(5) R(6) R(8) R(7)	HRRR_1	0.401	1.924	1.924	0.443
PV-001935350830	0.970	A(1) R(11) R(10) R(9)	ARRR_2	0.505	2.240	2.240	0.690
PV-001831793679	0.893	A(3) R(11) R(10) R(12)	ARRR_2	0.330	2.196	2.196	0.578
PV-001862316134	0.784	A(2) R(11) R(12) R(10)	ARRR_1	0.377	1.996	1.996	0.527
PV-001924736320	0.927	A(2) R(6) R(9) R(8)	ARRR_2	0.292	2.395	2.395	0.711
Z1545254023	0.971	H(6) R(8) R(7) R(9)	HRRR_1	0.446	2.128	2.128	0.529
PV-001925585102	0.934	A(1) R(8) R(7) R(9)	ARRR_1	0.476	2.177	2.177	0.641
Z2141883735	0.954	H(7) R(10) R(9) R(11)	HRRR_1	0.429	2.004	2.004	0.407
PV-001921223059	0.983	H(7) R(9) R(10) R(8)	HRRR_1	0.421	2.035	2.035	0.402
Z2770976320	0.877	A(3) R(9) R(10) R(8)	ARRR_2	0.438	2.162	2.162	0.650
Z2903058602	0.931	A(5) R(11) R(12) R(10)	ARRR_2	0.478	2.228	2.228	0.695
Z2193901479	0.766	A(2) R(12) R(11) R(13)	ARRR_2	0.346	2.085	2.085	0.607
Z2218766564	0.756	A(2) R(9) R(11) R(10)	ARRR_2	0.282	2.053	2.053	0.532
Z2903057141	0.978	A(2) R(9) R(11) R(12)	ARRR_1	0.966	1.902	1.902	0.728
PV-000817165047	0.868	A(1) R(8) R(7) R(9)	ARRR_1	0.331	2.137	2.137	0.545
Z2095183789	0.926	H(8) R(10) R(9) R(11)	HRRR_1	0.526	1.904	1.904	0.417
Z3188961853	0.843	A(2) R(8) R(7) R(9)	ARRR_1	0.495	1.919	1.919	0.489
Z2923423811	0.913	A(2) R(10) R(9) R(11)	ARRR_1	0.492	2.079	2.079	0.576
PV-002587460686	0.843	A(2) A(1) D(6) R(12) R(14)	AADRR_2	0.570	2.026	2.026	0.658
PV-001936869335	0.855	A(2) R(13) R(12) R(11)	ARRR_1	0.405	2.090	2.090	0.572
Z1498805014	0.911	A(2) R(11) R(10) R(12)	ARRR_1	0.711	1.858	1.858	0.540
Z1849714935	0.935	D(3) R(7) R(9) R(8)	DRRR_2	0.343	2.157	2.157	0.508
Z1753455598	0.840	D(7) R(10) R(12) R(11)	DRRR_2	0.537	1.876	1.876	0.484

All ligands were initially screened in high-throughput virtual screening (HTVS) mode and the top 10% of compounds were docked with Glide SP. Subsequently, the top 10% of compounds, but retaining only good score states, were processed by docking with Glide XP. At this stage, the default number of poses per compound state was increased to 5. Finally, 10% of the best compounds retaining only the best scoring states were obtained as output.

Sequential virtual screening including HTVS, SP and XP protocols allowed us to select a total of 2908 molecules which were then used for a Prime MM-GBSA analysis. After the Prime MM-GBSA analysis we selected molecules with energy lower than that of the co-crystallised ligand Fluconazole ( $\Delta G_{bind} = -25$  kcal/mol). To take into account the flexibility of the protein. The resulting set of molecules was subjected to the IFD protocol. The sequential virtual screening including HTVS, SP, XP, MM-GBSA prime and IFD protocols allowed us to select a total of 26 hits. Table 4 shows the 26 hits with their fitness scores and the pharmacophore models that were used to retrieve them during the virtual screening. The values of the fitness score parameter for the keys range from 1.858 to

2.395. The lead PV-001924736320 retrieved by the pharmacophoric model ARRR\_2 tops the list with a fitness score of 2.395 (Fig.3).

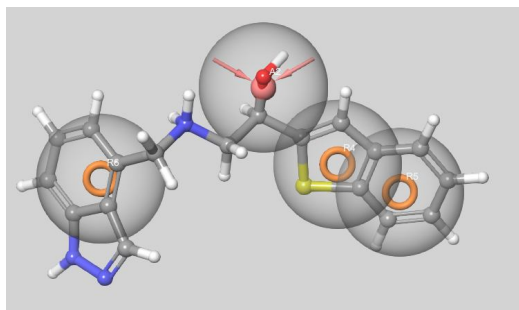


Fig.2. Lead PV-001924736320 aligned to pharmacophore model ARRR\_2

### 3.4 HTVS SP and XP analysis of hits

Table5. HTVS, SP, XP docking parameters of the obtained leads (in kcal/mol)

Touches	HTVS DOCKING			SP DOCKING			XP DOCKING		
	DOCKING SCORE	GLIDE ENERGY	GLIDE EMODEL	DOCKING SCORE	GLIDE ENERGY	GLIDE EMODEL	DOCKING SCORE	GLIDE ENERGY	GLIDE EMODEL
<b>Z1804044680</b>	-8.923	-47.714	-67.736	-11.140	-58.983	-93.243	-12.161	-53.130	-86.339
<b>PV-001850708261</b>	-9.456	-46.775	-73.427	-9.677	-54.878	-79.107	-10.841	-48.680	-84.414
<b>Z2283404606</b>	-9.319	-48.942	-68.945	-10.032	-51.520	-78.635	-10.885	-50.793	-87.113
<b>Z1651668373</b>	-5.962	-22.518	-17.878	-9.837	-52.321	-78.018	-10.970	-52.134	-88.625
<b>PV-001935350830</b>	-8.786	-41.495	-34.354	-10.757	-56.845	-91.132	-12.019	-56.954	-90.977
<b>PV-001831793679</b>	-9.122	-45.311	-64.560	-7.099	-53.391	-67.379	-10.848	-61.488	-87.027
<b>PV-001862316134</b>	-7.761	-27.803	-17.614	-9.564	-46.508	-64.530	-10.905	-48.342	-60.834
<b>PV-001924736320</b>	-9.551	-30.789	-47.971	-11.242	-56.392	-87.522	-12.041	-54.170	-77.241
<b>Z1545254023</b>	-9.998	-52.021	-81.670	-10.801	-55.752	-88.687	-11.193	-51.986	-83.211
<b>PV-001925585102</b>	-8.824	-32.728	-40.055	-10.086	-47.427	-76.576	-12.424	-52.759	-81.160
<b>Z2141883735</b>	-7.699	-44.061	-55.792	-9.715	-48.526	-71.436	-11.282	-49.391	-74.911
<b>PV-001921223059</b>	-9.157	-31.236	-35.499	-10.489	-53.756	-82.285	-10.824	-52.152	-72.417
<b>Z2770976320</b>	-7.583	-38.050	-48.510	-9.849	-55.290	-73.727	-11.244	-46.239	-79.568
<b>Z2903058602</b>	-10.149	-44.212	-69.213	-10.352	-49.524	-75.927	-11.118	-49.094	-70.696
<b>Z2193901479</b>	-8.672	-41.849	-56.768	-9.482	-52.299	-73.275	-10.843	-46.985	-74.904
<b>Z2218766564</b>	-7.974	-19.684	-16.882	-9.513	-50.575	-77.599	-11.028	-41.036	-71.238
<b>Z2903057141</b>	-9.331	-44.382	-67.541	-10.352	-49.524	-75.927	-10.783	-43.341	-63.562
<b>Z2095183789</b>	-8.378	-36.016	-54.355	-7.405	-46.934	-66.154	-11.793	-62.235	-97.029
<b>Z3188961853</b>	-7.226	-35.821	-34.572	-9.576	-57.547	-82.492	-11.026	-51.761	-72.321
<b>Z2923423811</b>	-8.736	-43.560	-64.569	-9.184	-47.100	-9.184	-11.282	-42.642	-77.004



PV-002587460686	-9.268	-33.162	-38.163	-9.826	-38.487	-9.826	-11.587	-50.164	-60.579
PV-001936869335	-7.811	-47.217	-69.068	-8.890	-56.669	-8.890	-11.303	-55.860	-91.769
Z1498805014	-9.093	-57.122	-92.983	-11.781	-60.787	-11.781	-11.352	-57.472	-102.095
Z1849714935	-8.903	-51.287	-79.031	-10.070	-47.795	-10.070	-11.492	-43.565	-80.866
PV-000817165047	7.972	-40.841	-57.472	-9.782	-56.276	-9.782	-11.410	-57.092	-97.470
Z1753455598	-7.579	-50.350	-68.082	-9.360	-59.338	-9.360	-11.822	-50.956	-88.870
fluconazole	-6.884	-33.107	-37.130	-5.684	-50.727	-67.499	-5.671	-49.571	-74.978

The results by docking glide HTVS, SP and XP of the hits are presented in Table 6. The values of the interaction energy parameters: docking score, glide energy and glide Emodel of the hits obtained by glide XP are between -10.783 and -12.424 kcal/mol; -41.036 and -62.235 kcal/mol; -60.579 and -102.095 kcal/mol respectively. The docking score values of the leads in the different methods HTVS, SP and XP are lower than those of fluconazole. Therefore, these 26 leads have a higher affinity than the reference molecule, which confers a better stability in the active site of the 1EA1 protein target..

### 3.5 Prime MM-GBSA analysis of hits

The Prime/MM-GBSA method based on the complex obtained after Docking XP was used to calculate the free enthalpy of binding  $\Delta G_{bind}$  of the ligands in the active site of the target protein 1EA1 and the results obtained are summarised in Table 7.

The free enthalpy of binding  $\Delta G_{bind}$  of the leads ranges from -61.03 to -20.45 kcal/mol. According to the energy components of the free enthalpies of binding given in Table 7, the main favourable energetic factors for ligand binding are van der Waals interactions  $\Delta G_{vdw}$  (ranging from -34.98 to -57.334 kcal/mol), electrostatic or coulomb interactions  $\Delta G_{coulomb}$  (ranging from -0.41 to -98.92 kcal/mol) and lipophilic interactions  $\Delta G_{lipo}$  (ranging from -17.417 to -44.71 kcal/mol). Except for the leads Z2903058602 ( $\Delta G_{covalent} = -0.79$  kcal/mol) and Z3188961853 ( $\Delta G_{covalent} = -0.384$  kcal/mol) whose covalent interaction energy terms  $\Delta G_{covalent}$  contribute favourably to the free enthalpy of bonding, the other leads have a contribution of  $\Delta G_{covalent}$  (between 1.69 and 21.77 kcal/mol) unfavourable to ligand binding. The solvation interaction energy terms  $\Delta G_{solvGB}$  (ranging from 38.15 to 124.83 kcal/mol) are significantly unfavourable to ligand binding. Furthermore, apart from the leads Z3188961853, Z2283404606 and Z1753455598, it is evident that the contribution of the hydrogen bonding energy  $\Delta G_{H-bond}$  (ranging from -2.53 to 1.26 kcal/mol) and the packing energy  $\Delta G_{packing}$  (ranging from -0.371 to -8.95 kcal/mol) is small in the free enthalpy of binding. Furthermore, the high negative values of  $\Delta G_{vdw}$  and  $\Delta G_{lipo}$  indicate the presence of massive hydrophobic interactions between the *candida albicans* enzyme and the hits obtained. Except for **Z2405188545**, the hits obtained have lower free enthalpies of binding  $\Delta G_{bind}$  than that of the reference ligand ( $\Delta G_{bind} = -28.178$  kcal/mol). These results indicate that the hits obtained are suitable for the active site of the *candida albicans* (1EA1) enzyme.

Table 6. Prime MM-GBSA analysis of the hits.

Touches	$\Delta G_{bind}$	$\Delta G_{coulomb}$	$\Delta G_{covalent}$	$\Delta G_{H-bond}$	$\Delta G_{lipo}$	$\Delta G_{packing}$	$\Delta G_{solvGB}$	$\Delta G_{vdw}$
<b>Z1804044680</b>	-48.53	-48.29	7.76	-0.69	-35.37	-4.13	77.91	-45.72
<b>PV-001850708261</b>	-32.054	-21.371	7.578	-0.742	-17.417	-2.568	50.925	-48.459
<b>Z2283404606</b>	-37.162	-34.643	2.090	0.558	-26.944	-0.371	79.064	-56.916
<b>Z1651668373</b>	-58.79	-63.57	9.81	-0.72	-33.44	-5.73	82.36	-47.51
<b>PV-001935350830</b>	-44.46	-16.90	7.72	-1.85	-21.90	-7.04	46.98	-51.48
<b>PV-001831793679</b>	-41.87	-31.00	17.41	-2.03	-44.71	-7.07	72.41	-46.88
<b>PV-001862316134</b>	-28.71	-28.72	9.16	-0.99	-37.22	-7.92	71.96	-34.98

<b>PV-001924736320</b>	-37.51	-53.21	6.23	-0.64	-26.65	-7.50	89.57	-45.31
<b>Z1545254023</b>	-52.01	-70.64	6.45	-1.34	-24.97	-4.81	92.80	-49.51
<b>PV-001925585102</b>	-38.59	-61.77	7.10	-1.28	-26.17	-5.24	95.01	-46.24
<b>Z2141883735</b>	-43.43	-22.43	8.07	-0.73	-31.41	-4.09	50.38	-43.22
<b>PV-001921223059</b>	-51.00	-62.96	8.26	-1.38	-40.26	-4.30	91.29	-41.65
<b>Z2770976320</b>	-45.76	-20.16	11.83	-1.31	-23.00	-6.19	38.15	-45.08
<b>Z2903058602</b>	-32.74	-6.32	-0.79	-0.67	-22.88	-6.87	48.02	-43.23
<b>Z2193901479</b>	-31.67	-12.54	9.65	-0.58	-23.36	-6.13	48.98	-47.68
<b>Z2218766564</b>	-53.99	-61.21	5.94	-0.88	-36.42	-5.79	84.33	-39.97
<b>Z2903057141</b>	-30.42	-12.89	2.72	-0.75	-21.31	-7.29	45.28	-36.18
<b>Z2095183789</b>	-39.62	-35.04	1.69	-1.78	-25.99	-4.53	75.04	-49.01
<b>Z3188961853</b>	-40.144	-44.289	-0.384	0.038	-21.320	-3.717	77.583	-48.056
<b>Z2923423811</b>	-47.50	-26.16	3.04	-1.87	-32.48	-5.04	62.15	-47.14
<b>PV-002587460686</b>	-20.45	-36.38	21.77	-1.81	-33.23	-5.43	78.45	-43.83
<b>PV-001936869335</b>	-41.22	-26.50	3.73	-1.82	-31.59	-5.45	67.73	-47.32
<b>Z1498805014</b>	-61.03	-64.86	8.13	-2.53	-37.16	-4.98	92.79	-52.42
<b>Z1849714935</b>	-53.96	-98.92	7.31	-0.92	-34.44	-5.60	124.83	-46.23
<b>PV-000817165047</b>	-41.93	-64.04	8.50	-0.81	-38.13	-8.95	116.55	-55.05
<b>Z1753455598</b>	-25.725	-0.410	7.476	1.126	-31.513	-4.899	59.830	-57.334
<b>fluconazole</b>	-28.178	-2.588	-1.731	-0.103	-18.113	-8.708	43.713	-40.648

---


$$\Delta G_{bind} = \Delta G_{coulomb} + \Delta G_{covalent} + \Delta G_{H-bond} + \Delta G_{lipo} + \Delta G_{packing} + \Delta G_{solGB} + \Delta G_{wdw}$$

### 3.6 IFD analysis of hits

The parameters glide energy, glide Emodel, docking score and IFD score as well as the different types of interactions between the hits obtained and the residues of the active site of the 1EA1 protein are summarised in Table .8. The parameters glide energy, glide Emodel, docking score and IFD score as well as the different types of interactions between the hits obtained and the residues of the active site of the 1EA1 protein are summarised in Table IV.8. The docking score, IFD score, glide Emodel, glide energy parameters of the hits obtained are between -14.041 and -10.229 kcal/mol ; -985.918 and -978.162 kcal/mol ; -112.728 and -75.456 kcal/mol ; -63.187 and -44.602 kcal/mol respectively.

**Table7.IFD Analysis of the hits compounds**

Hits	Glide Energy	Glide Emodel	Docking Score	Ifdscore	Hydrogen-bond interaction	Hydrophobic interaction	Interaction Pi-Pi ,Pi-Cation,Salt Bridge
<b>Z1804044680</b>	-57.589	-92.654	-12.718	-982.873	His259,val435	, Tyr76, Phe78, Met79, Phe83, Leu100, Phe255, Ala256, Leu321, Met433, Val434	Tyr76 <sup>a</sup> , phe78 <sup>a,b</sup> , hem460 <sup>b</sup>
<b>PV-001850708261</b>	-52.992	-76.704	-10.799	-983.980	Thr260, gln72	Tyr76, Phe78, Met79, Phe255, Leu321	Hem460 <sup>a</sup> , tyr76 <sup>a</sup>
<b>Z2283404606</b>	-61.114	-108.122	-13.504	-982.746	val435 , his259	Tyr76, Phe78, Met79, Phe83, Met99, Leu100, Phe255, Ala256, Leu321, Val434	Phe78 <sup>a</sup> ,tyr76 <sup>a</sup>
<b>Z1651668373</b>	-62.123	-96.840	-12.442	-982.017	Thr260, his259	Tyr76, Phe78, Met79, Phe83, Leu100, Phe255, Ala256, Leu321	Hem460 <sup>b,c</sup> , phe78 <sup>a</sup>
<b>PV-001935350830</b>	-60.930	-100.715	-11.685	-981.866	Ile323, pro320,val435	Tyr76, Phe78, Met79, Phe83, Phe255, Ala256, Leu321, Val434,	Phe78 <sup>a</sup> , hem460 <sup>a</sup>
<b>PV-001831793679</b>	-61.382	-108.534	-12.787	-981.467	His259, ile323, val435	Tyr76, Phe78, Met79, Phe83, Leu100, Phe255, Leu321, Ile322, Ile323, Met433, Val434	Phe78 <sup>a</sup> , Tyr76 <sup>a</sup>
<b>PV-001862316134</b>	-60.603	-98.435	-12.384	-981.223	Ala256, thr260	Tyr76, Phe78, Met79, Met99, Leu100, Phe255, Ala256, Leu321	Hem460 <sup>a,b</sup>
<b>PV-001924736320</b>	-62.682	-99.808	-13.786	-981.078	Arg95, ser252	Tyr76, Phe78, Met79, , Met99, Leu100, Phe255, Ala256, Leu321	Phe83 <sup>a</sup> , phe78 <sup>a</sup> ,hem460 <sup>b,c</sup>
<b>Z1545254023</b>	-51.409	-87.496	-11.648	-980.913	His259, thr260, val435	Tyr76, Phe78, Met79, Phe83, Phe255, Ala256, , Leu321, Ile323, Val434	Phe78 <sup>a</sup> , Tyr76 <sup>a,b</sup> Hem460 <sup>b,c</sup>
<b>PV-001925585102</b>	-52.422	-87.198	-12.085	-980.654	His259, val435	Tyr76, Phe78, Met79, Phe83, Met99, Leu100, Phe255, Ala256, Leu321, ,Val434	Phe78 <sup>a</sup> , Tyr76 <sup>a,b</sup> Hem460 <sup>b</sup>
<b>Z2141883735</b>	-55.633	-90.514	-11.834	-980.457	His259, thr260, val435	Tyr76, Phe78, Met79, Phe255, Ala256, , Leu321, Val434	Phe78 <sup>a</sup> , Tyr76 <sup>a</sup> Hem460 <sup>a</sup>

<b>PV-001921223059</b>	-58.625	-91.232	-13.259	-980.317	His259, thr260	Tyr76, Phe78, Met79, Phe83, Leu100, Ala256, Leu321, Ile323, Met433, Val434,Leu324	Phe78 <sup>a</sup> , Tyr76 <sup>a</sup> Arg96 <sup>b</sup> ,Hem460 <sup>b,c</sup>
<b>Z2770976320</b>	-58.503	-96.359	-11.560	-980.065	Ser252, val435, his259	Tyr76, Phe78, Met79, Phe83, , Met99, Leu100, Phe255, Leu321	Phe78 <sup>a</sup>
<b>Z2903058602</b>	-56.000	-80.798	-11.551	-979.947	His259, val435	Tyr76, Phe78, Met99, Leu100, Leu321, Ile323, Met433, Val434	Tyr76 <sup>a</sup> ,phe78 <sup>a</sup> ,phe83 <sup>a</sup>
<b>Z2193901479</b>	-54.583	-90.923	-10.680	-979.841	Thr260,ala256	Tyr76, Phe78, Met79, Phe83, Met99, Leu100, Phe255, Ala256, Leu321, Val434	Hem460 <sup>a,b</sup>
<b>Z2218766564</b>	-60.258	-104.094	-11.573	-979.509	Arg95,His259,thr260	Tyr76, Phe78, Met79, Phe83, Leu100, Phe255, Ala256, Leu321, Val434	Phe78 <sup>a</sup> ,Hem460 <sup>b</sup>
<b>Z2903057141</b>	-44.602	-75.456	-10.229	-979.264	Met433	Tyr76, Phe78, Met79, Phe83, Met99, Leu100, Phe255, Ala256, Leu321, Ile322, Ile323	Phe78, hem460
<b>PV-000817165047</b>	-60.296	-94.087	-11.762	-978.162	Val435	Tyr76, Phe78, Phe255, Leu321, Ile323, Met325	Phe78 <sup>a</sup> , hem460 <sup>a,c</sup>
<b>Z2095183789</b>	-63.187	-112.728	-13.066	-985.918	Val435	Gln72, Tyr76, Phe78, Met79, Phe83, Arg95, Arg96, Met99, Leu100, Phe255, Ala256, His259, Thr260, Leu321, Ile322, Ile323, Met325 Met433, Val434,Leu324	Phe78 <sup>a</sup> , hem460 <sup>a,c</sup>
<b>Z3188961853</b>	-56.528	-97.253	-11.305	-978.450	Met433	Tyr76, Phe78, Met79, Phe83, Met99, Leu100, Phe255, Ala256, Leu321, Ile323, Met433, Val434	Tyr76 <sup>a</sup> , phe78 <sup>a</sup>
<b>Z2923423811</b>	-62.538	-106.940	-14.041	-983.891	Ile323, his259, val435	Tyr76, Phe78, Met79, Met99, Leu100, Phe255, Ala256, Leu321, Val434	Phe78 <sup>a</sup>
<b>PV-002587460686</b>	-60.672	-100.510	-11.723	-983.860	Arg95, arg96, hem460, his259	Tyr76, Phe78, Met79, Phe83, Phe255, Ala256, Leu321, Ile323, Met325 Met433	Tyr76 <sup>a</sup> , hem460 <sup>a</sup>
<b>PV-001936869335</b>	-58.959	-95.643	-11.608	-981.634	Met433, arg95, ser252	Tyr76, Phe78, Met79, Phe83, Met99, Leu100, ser252 Phe255,	Phe78 <sup>a</sup> , hem460 <sup>a</sup>

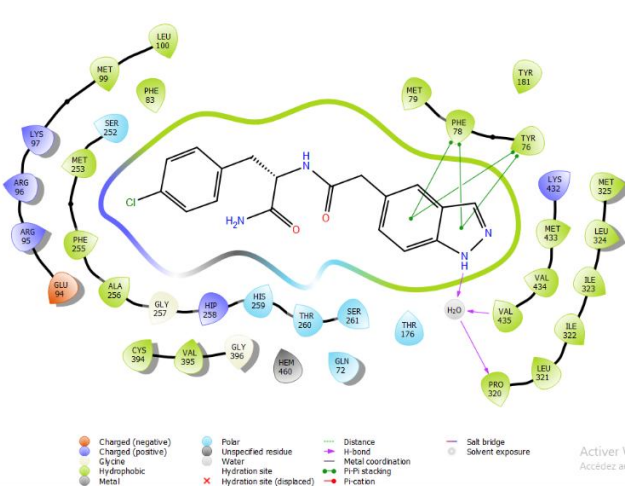
						Ala256, Leu321, Val434	
<i>Z1498805014</i>	-61.361	-99.213	-12.218	-980.572	Arg95, met433	Tyr76, Phe78, Met79, Phe83, Leu100, Phe255, Ala256, Leu321, Ile323, Val434	Hem460 <sup>b,c</sup>
<i>Z1849714935</i>	-58.599	-95.006	-11.390	-979.448	His259, thr260	Tyr76, Phe78, Met79, Phe83, Met99, Leu100, Phe255, Leu321, Val434	Phe78, hem460 <sup>b,c</sup>
<i>Z1753455598</i>	-59.452	-91.648	-11.862	-976.845	Thr260	Tyr76, Phe78, Met79, Phe83, Met99, Leu100, Phe255, Leu321, Val434	Phe78 <sup>a</sup> , Arg95 <sup>b</sup> , Hem460 <sup>b</sup>
<i>FLUCONAZOLE</i>	-49.029	-72.175	-7.158	-977.380	His259,thr260	Tyr76, Phe78, Met79, Phe83,Phe255, Leu321	Hem460 <sup>a</sup>

a : pi-pi interaction

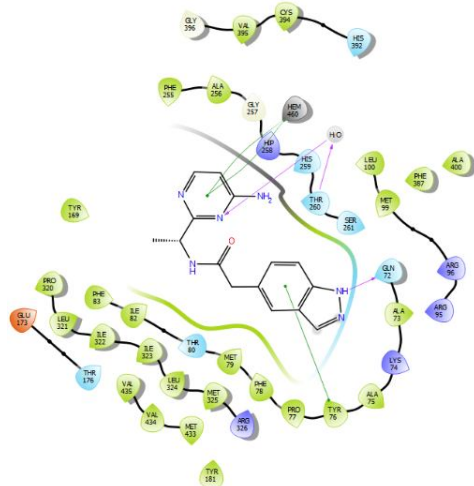
b :pi-cation interaction

c :interaction salt bridge

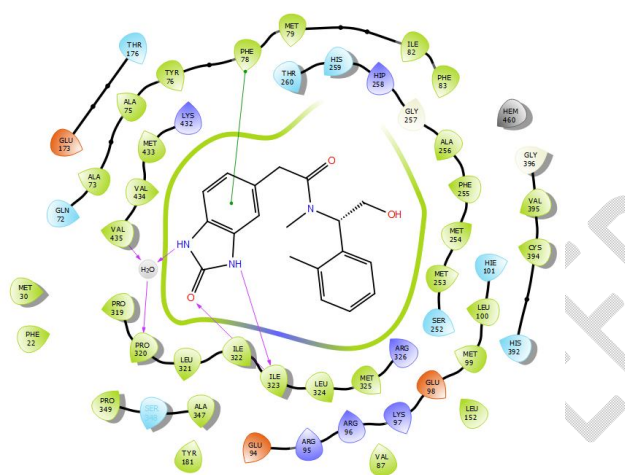




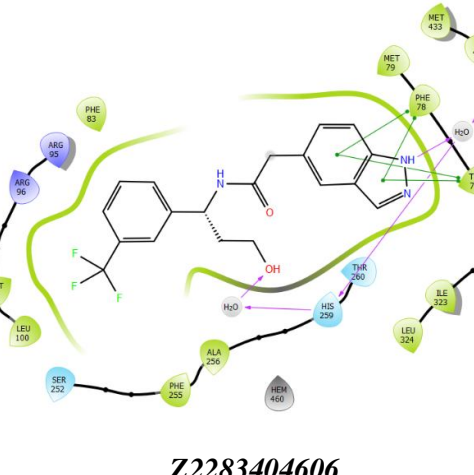
**Z2095183789**



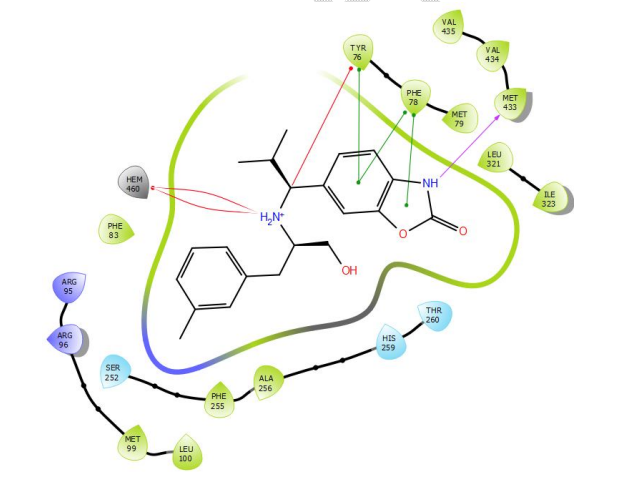
**PV-001850708261**



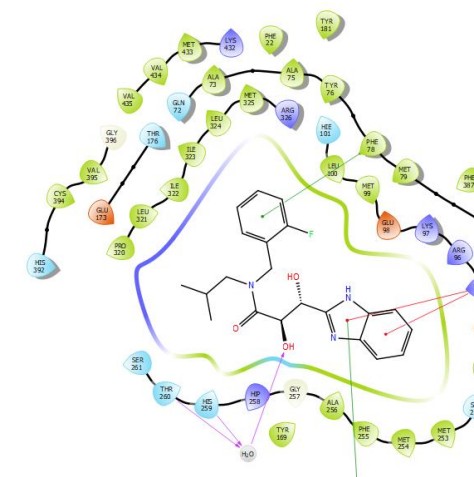
**Z2923423811**



**Z2283404606**



**Z1804044680**



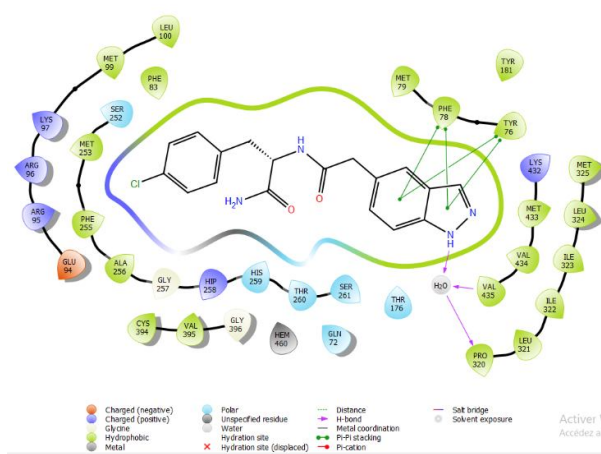
**Z1753455598**

**Fig.3: Interactions of hits with the lowest IFD scores.**

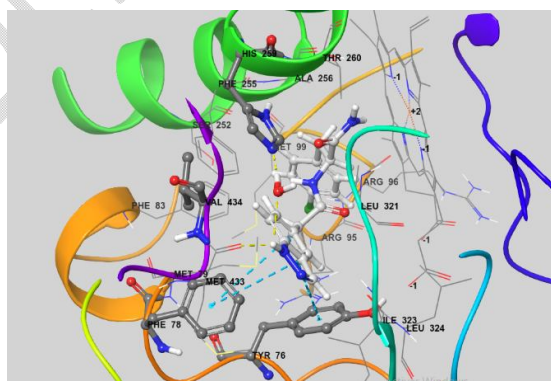
Fig.4 illustrates the interactions of the HITS **Z2283404606**, **Z1804044680**, **Z2923423811**, **PV-001850708261**, **Z2095183789** which have the lowest IFDscore as well as the lead Z1753455598 which has the highest IFDscore with residues of the *candida albicans* active site. The binding modes of the leads with the lowest IFDscore (**Z2923423811**, **PV-001850708261**, **Z2095183789**) as well as the one with the highest IFDscore (**Z1753455598**) were discussed in detail.

- **Binding mode of Z2095183789**

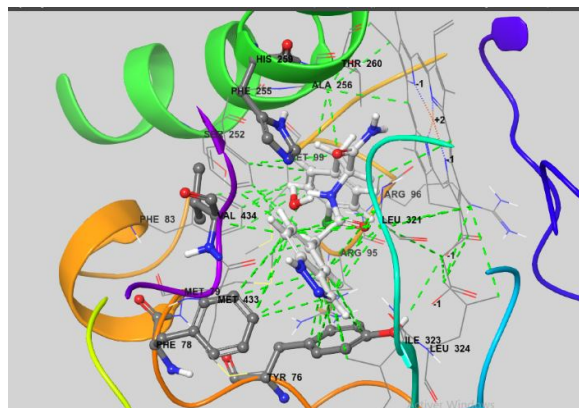
The lead **Z2095183789** has an IFDscore of -985.918kcal/mol and a considerably low docking score of -13.066kcal/mol, which is lower than that of the standard co-crystallised ligand (IFDscore= -977.380kcal/mol ; Dockingcore= -7.158 kcal/mol). The lead **Z2095183789** binds to the 1EA1 receptor active site by forming four hydrogen bonds, a direct hydrogen bond with residue Met433 and hydrogen bonds via a water molecule with residues Val435, Pro320 and His259 of the active site (Fig.5 and 6). The first hydrogen bond is established between the oxygen of the carbonyl group c=O of residue Met433 and a hydrogen atom of the 2-pyrazoline heterocycle of the ligand with the parameters ( $d(H\cdots Y)=1.90 \text{ \AA}$  ;  $d(X\cdots Y)=2.83 \text{ \AA}$  ;  $\angle XHY=151.6^\circ$ ).



**Fig. 4 : Binding mode of the hitZ2095183789**



**Fig.5.3D binding mode of the hit Z2095183789 in the active site of 1EA1(hydrogen bonding: yellowcolour; pi-pi interaction: blue colour**

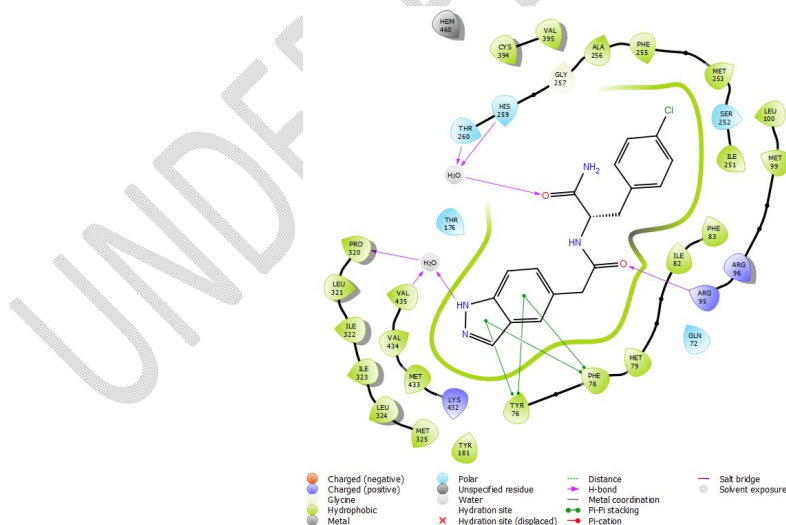


**Fig.6. Hydrophobic interactions of the hit Z2095183789 with the active site residues of 1EA1.**

Three hydrogen bonds are formed between a hydrogen atom of the pyrazoline ring and residues Val435, Pro320 and His259 via a water molecule with the following hydrogen bond parameters (ligand-H<sub>2</sub>O :  $d(H \cdots Y)=2.63 \text{ \AA}$ ,  $d(X \cdots Y)=3.29 \text{ \AA}$   $\angle XHY=123.3^\circ$ ; H<sub>2</sub>O-Val435 :  $d(H \cdots Y)=1.93 \text{ \AA}$ ,  $d(X \cdots Y)=2.93 \text{ \AA}$   $\angle XHY=169.2^\circ$ ; H<sub>2</sub>O-Pro320 :  $d(H \cdots Y)=1.71 \text{ \AA}$ ,  $d(X \cdots Y)=2.72 \text{ \AA}$   $\angle XHY=173.7^\circ$  H<sub>2</sub>O-His259 :  $d(H \cdots Y)=1.80 \text{ \AA}$ ,  $d(X \cdots Y)=2.80 \text{ \AA}$   $\angle XHY=174.7^\circ$ ).

Furthermore we found that the indazole ring establishes two pi-pi bonds with residues Tyr76 and Phe78. In addition the compound Z2095183789 shows hydrophobic interactions with residues Tyr76, Phe78, Met79, Phe83, Met99, Phe255, Ala256, Leu321, Ile323, Val434, (Fig.7) which allows the fixation of the ligand in the active site of the enzyme.

Also we presented in Fig.8 another pose of the lead Z2095183789 (IFDscore= -984.728 kcal/mol ; Dockingscore= -12.435 kcal/mol) in order to highlight the possibility of the latter to form hydrogen bonds with residues Thr260 and His259 of the active site like fluconazole.



**Fig.7. Binding mode of the lead Z2095183789 with interaction with Thr260 and His259**

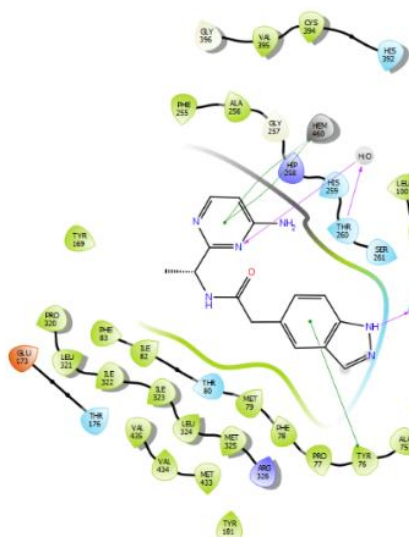
- **Binding mode of PV-001850708261**

The molecule *PV-001850708261* has an IFDscore and a docking score of -10.799 kcal/mol, which is lower than that of the co-crystallized ligand. It forms two hydrogen bonds with the residues **Gln72**

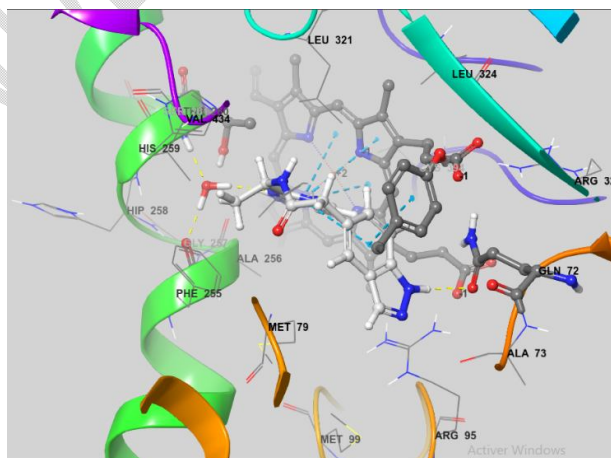


and **Thr260** in the active site of receptor **1EA1** (Fig. 9 and 10), with the following geometric parameters: **Gln72** ( $d(H \cdots Y) = 2.06 \text{ \AA}$ ,  $d(X \cdots Y) = 3.00 \text{ \AA}$ ,  $\angle XHY = 153.10^\circ$ ); **Thr260 (ligand-H2O)**:  $d(H \cdots Y) = 2.16 \text{ \AA}$ ,  $d(X \cdots Y) = 3.17 \text{ \AA}$ ,  $\angle XHY = 171.40^\circ$  **H2O – Thr260**:  $d(H \cdots Y) = 1.92 \text{ \AA}$ ;  $d(X \cdots Y) = 2.93 \text{ \AA}$ ;  $\angle XHY = 178.3^\circ$ ).

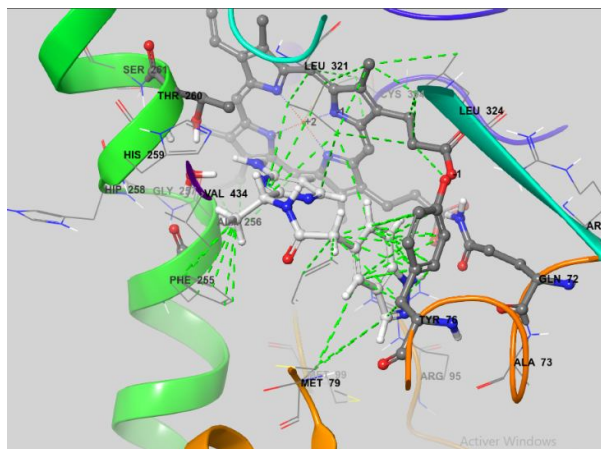
Furthermore, the molecule PV-001850708261 interacts with residues **Tyr76** and **Hem460** through **pi-pi** and **pi-cation** interactions, respectively. Additionally, PV-001850708261 forms hydrophobic interactions with **Tyr76**, **Phe78**, **Met79**, **Phe255**, and **Leu321** in the active site of the protein (Fig.11).



**Fig.8: Binding mode of the hit PV-001850708261**



**Fig.10 : Binding mode of the hit PV-001850708261 in the active site of 1EA1**



**Fig.11.** Hydrophobic interactions of the hit PV-001850708261 with the residues in the active site of 1EA1

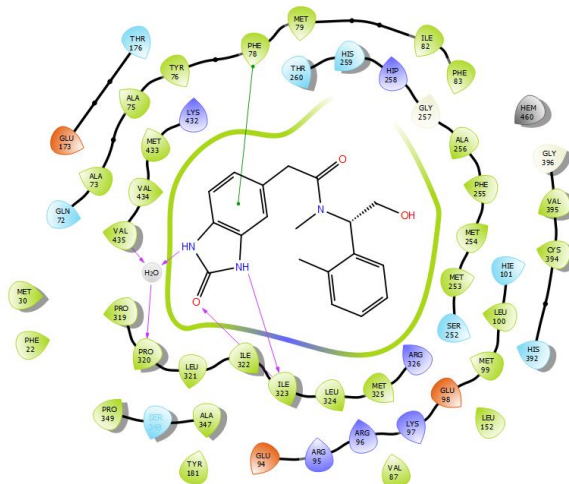
- **Binding mode of Z2923423811**

Z2923423811 has an IFDscore of -983.891kcal/mol and a Docking score of -11.723kcal/mol, lower than that of fluconazole. It binds to the active site of the protein target by forming four hydrogen bonds with residues Ile323, His259, Val435, Pro320 and a pi-pi interaction with residue Phe78 (Fig.12 and13). The geometric parameters of the different hydrogen bonds are as follows: **Ile322** ( $d(H \cdots Y)=2.15 \text{ \AA}$ ,  $d(X \cdots Y)=3.15 \text{ \AA}$ ,  $\angle XHY=167^\circ$ ); **Ile323** ( $d(H \cdots Y)=1.88 \text{ \AA}$ ,  $d(X \cdots Y)=3.00 \text{ \AA}$ ,  $\angle XHY=153.10^\circ$ );

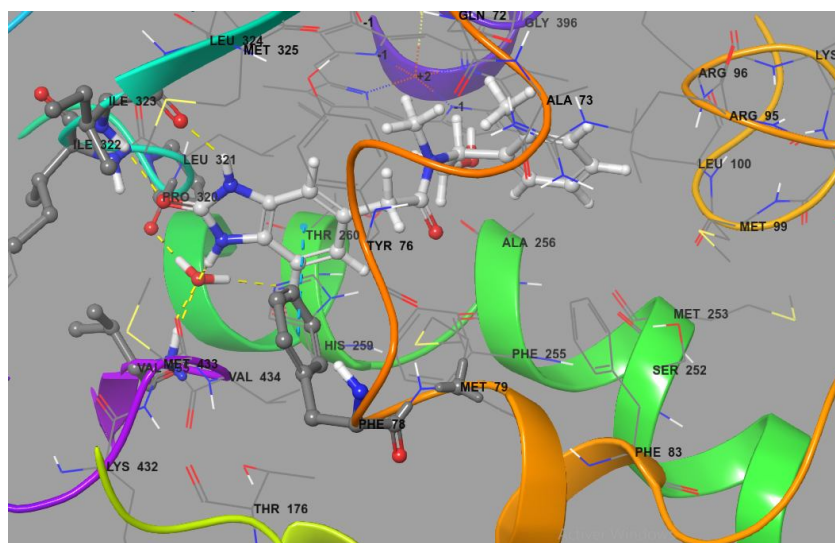
**Val435, Pro320** (ligand-H<sub>2</sub>O: $d(H \cdots Y) = 2.12 \text{ \AA}$ ,  $d(X \cdots Y) = 2.98 \text{ \AA}$ ,  $\angle XHY = 141.70^\circ$ )

**H<sub>2</sub>O – Pro320**:  $d(H \cdots Y) = 1.71 \text{ \AA}$ ;  $d(X \cdots Y) = 2.72 \text{ \AA}$ ;  $\angle XHY = 175.6^\circ$ .

**H<sub>2</sub>O – Val435**:  $d(H \cdots Y) = 1.87 \text{ \AA}$ ;  $d(X \cdots Y) = 2.86 \text{ \AA}$ ;  $\angle XHY = 162.7^\circ$ .

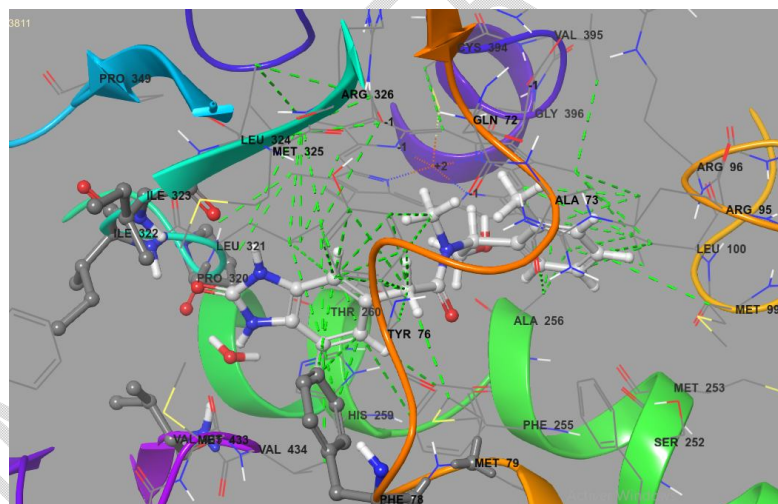


**Fig.9.** Binding mode of the hit Z2923423811



**Fig.10. 3D binding mode of the hit Z2923423811 in the active site of 1EA1**

Furthermore, the molecule Z2923423811 forms hydrophobic interactions with the residues **Tyr76**, **Phe78**, **Met79**, **Met99**, **Leu100**, **Phe255**, **Ala256**, **Leu321**, and **Val434** in the active site (Fig 14).



**Fig.11. Hydrophobic interactions of the hit Z2923423811 with the residues in the active site of 1EA1**

- **Binding mode of Z1753455598**

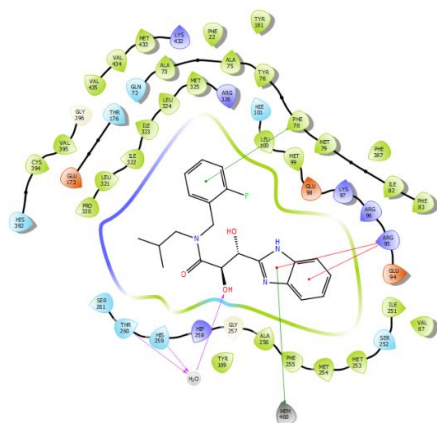
Regarding the molecule **Z1753455598**, it has the highest IFDScore among the identified molecules. This parameter is slightly higher than that of the co-crystallized ligand (Fluconazole: IFDScore = -977.380 kcal/mol; Docking Score = -7.158 kcal/mol). **Z1753455598** binds to the active site by forming two hydrogen bonds with residues Thr260 and His259 through a water molecule (Fig .15 and .16) with the following geometric parameters:

**Ligand-H2O:**  $d(H \cdots Y) = 1.88 \text{ \AA}$ ,  $d(X \cdots Y) = 2.87 \text{ \AA}$ ,  $\angle XHY = 167.90^\circ$

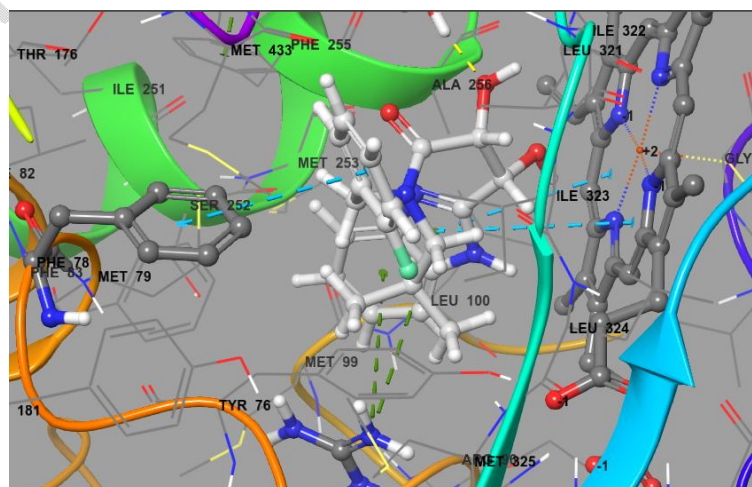
**H2O – His259:**  $d(H \cdots Y) = 1.62 \text{ \AA}$ ;  $d(X \cdots Y) = 2.64 \text{ \AA}$ ;  $\angle XHY = 166.7^\circ$

**H2O – Thr260:**  $d(H \cdots Y) = 2.22 \text{ \AA}$ ;  $d(X \cdots Y) = 3.23 \text{ \AA}$ ;  $\angle XHY = 171^\circ$ ,

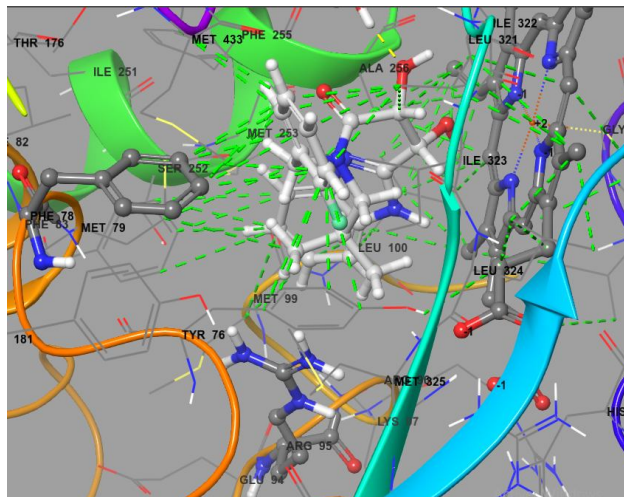
The molecule Z1753455598 also forms pi-cation interactions with residue Arg95 and pi-pi interactions with residue Phe78 and the heme molecule (HEM450) in the active site. The visualization of the 3D docking pose (Fig.17) shows that compound Z1753455598 establishes several hydrophobic interactions with active site residues, including Tyr76, Phe78, Met79, Phe83, Met99, Leu100, Phe255, Leu321, and Val434.



**Fig.12.Binding mode of the hit Z1753455598.**



**Fig.13.3D binding mode of the molecule Z1753455598 in the active site of 1EA1**



**Fig.14. Hydrophobic interactions of the molecule Z1753455598 with the residues in the active site of 1EA1**

Except for the molecule Z2723048448, all ligands have **IFDscore** and **Docking score** parameters lower than those of fluconazole. Similarly, the docking pose analysis of the molecules revealed that they form hydrogen bonds, **pi-pi**, **pi-cation**, and hydrophobic interactions with the residues of the active site, similar to those of the reference ligand. The predominant protein-ligand interactions in the different poses are the hydrophobic interactions. Other molecules exhibit additional hydrogen bonds. The binding mode via **IFD** presented above shows that these different molecules are strong candidates for the inhibition of *Candida albicans* and could be further optimized to improve their activity profile.

### 3.7 Prediction of ADME parameters

The ADME properties (Absorption, Distribution, Metabolism, and Excretion) of the top 26 ranked compounds were evaluated using the **QikProp** tool integrated into Schrödinger software. These compounds stand out due to their excellent **QPlogPo/w**, **QPlogS**[37] values, molecular weight, as well as the number of hydrogen bond donors and acceptors, **QPlogBB**, and their percentage of human oral bioavailability, all fully compliant with Lipinski's rule of five [38] (Table 8). Furthermore, features such as a reduced polar surface area, high oral bioavailability, and an optimal number of hydrogen bond donors and acceptors are critical factors for the development of therapeutic agents. The results in table 5 also indicates that these compounds exhibit Caco-2 cell permeability (**QPCCaco**) within an acceptable range (>70), reflecting adequate absorption and distribution of the molecules studied. Additionally, the top hits show high human oral absorption (**% HOA**) values ranging from 63 to 100%. Overall, the parameters of the analysed compounds meet the criteria outlined by Lipinski's rule of five, confirming their potential as therapeutic candidates in this study.

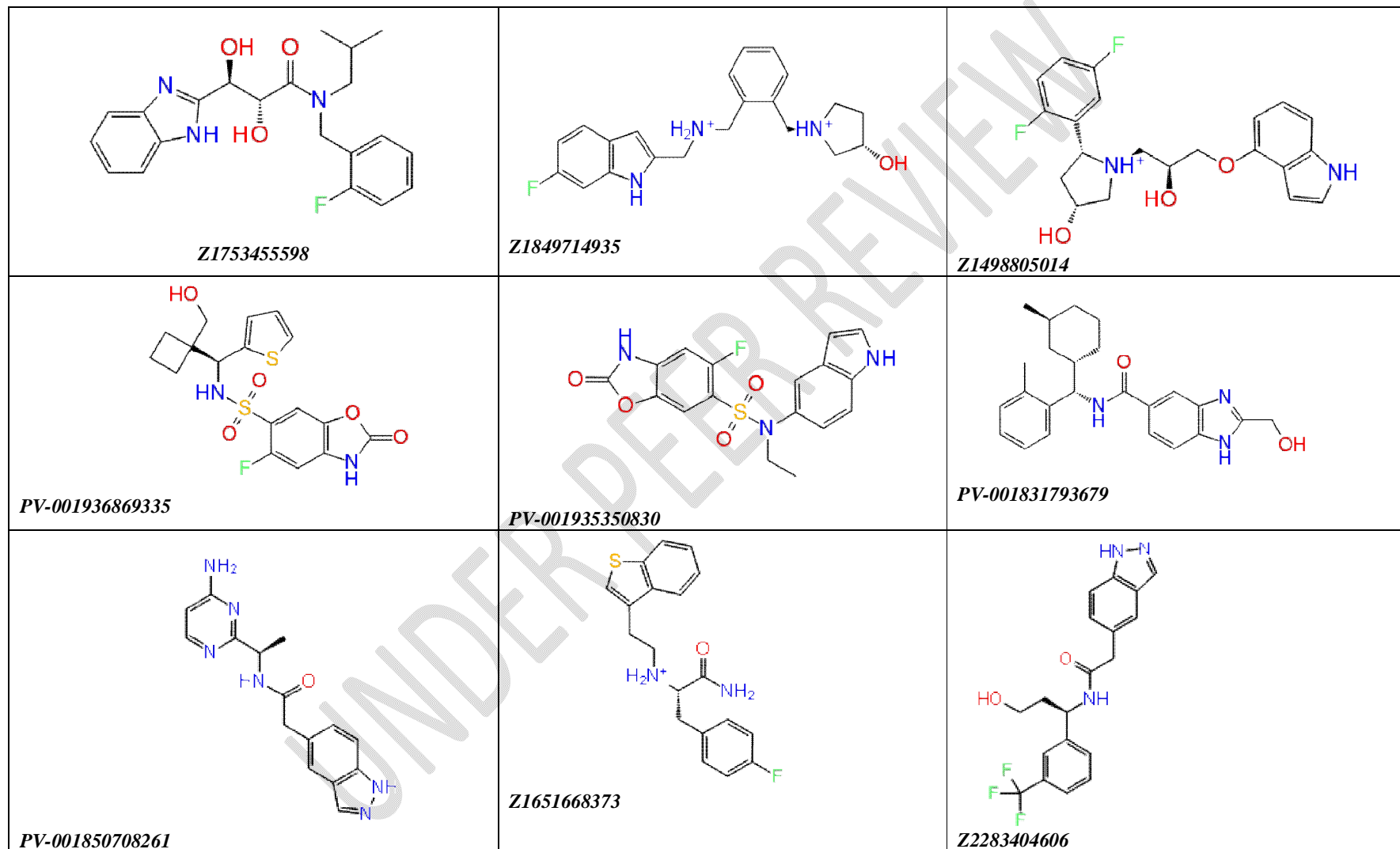
UNDER PEER REVIEW

**Table 8 : ADME properties of the hits**

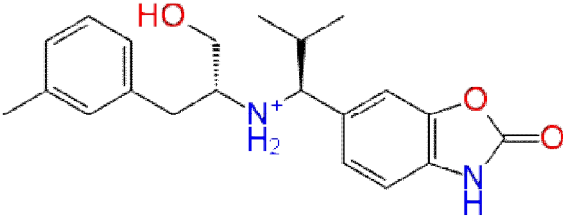
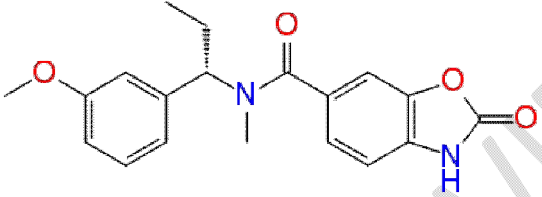
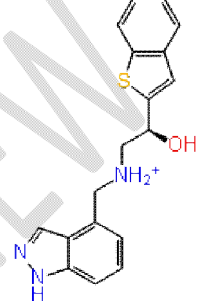
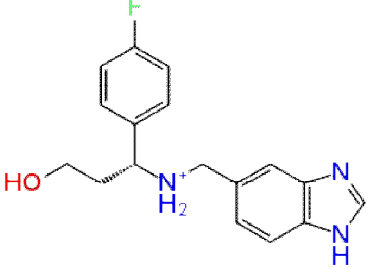
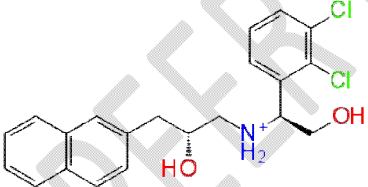
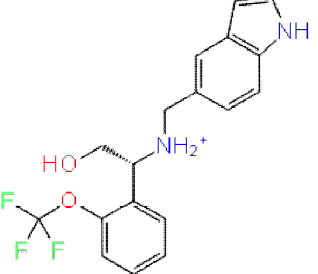
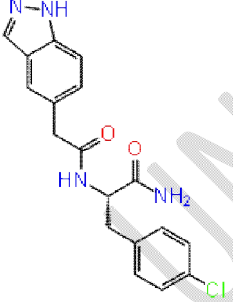
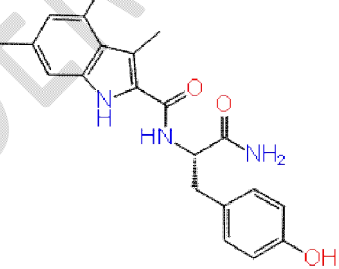
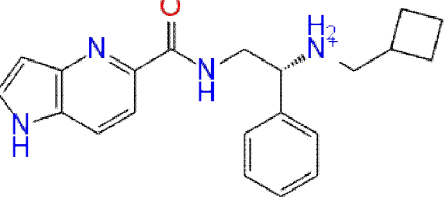
Hits	MW	donor HB	Acpt HB	QPlogPw	QPlogPo/w	QPlogS	QPPCaco	Human Oral Absorption(HOA)	Percent Human Oral Absorption	QPlog BB	QPlogKhsa	PSA	QPPMDCK	Rule Of Five
Z1753455598	385.437	2.000	6.900	13.314	3.131	-3.952	851.982	3	100.000	-0.847	-0.135	88.663	882.286	0
Z1849714935	353.438	3.000	5.200	11.570	2.665	-1.560	119.567	3	79.735	0.407	0.237	53.168	110.349	0
Z1498805014	388.413	3.000	6.150	13.250	3.204	-3.883	209.810	3	87.261	-0.407	0.265	67.747	246.549	0
PV-001936869335	412.450	3.000	9.200	15.425	1.110	-2.698	115.007	3	70.329	-1.400	-0.350	120.563	86.578	0
PV-001935350830	375.374	2.000	7.500	13.696	1.655	-3.712	155.446	3	75.859	-1.372	-0.141	107.608	84.567	0
PV-001831793679	391.512	3.000	5.700	12.761	4.118	-6.087	575.988	3	100.000	-1.157	0.657	84.425	272.512	0
PV-001850708261	296.331	4.000	6.000	17.195	0.858	-2.555	89.151	3	66.870	-1.562	-0.512	115.171	68.937	0
Z1651668373	342.430	3.000	4.000	13.276	3.103	-2.771	219.261	3	87.014	-0.035	0.030	59.664	688.981	0
Z2283404606	377.365	3.000	5.700	14.544	2.268	-2.862	205.131	3	81.607	-0.998	-0.220	87.662	414.153	0
Z1804044680	354.448	3.000	6.200	12.316	2.480	-3.007	112.569	3	78.182	-0.850	0.190	89.007	51.633	0
Z2141883735	340.378	1.000	6.750	10.553	2.811	-4.288	672.074	3	94.009	-0.881	0.022	89.282	321.965	0
PV-001924736320	323.412	3.000	4.200	11.768	2.907	-3.436	190.101	3	84.754	-0.504	0.158	65.662	139.353	0
Z1545254023	299.347	3.000	4.700	11.530	2.372	-2.810	161.927	3	80.374	-0.544	-0.028	64.211	128.162	0
PV-001921223059	390.308	3.000	4.900	10.808	3.211	-2.292	323.035	3	90.657	-0.134	0.173	51.642	453.509	0
PV-001925585102	350.340	3.000	3.200	9.652	3.295	-2.640	361.479	3	92.024	0.064	0.228	54.634	704.614	0
Z2095183789	356.811	3.250	5.250	17.535	1.093	-1.124	47.951	2	63.427	-1.184	-0.576	116.357	143.501	0
PV-002587460686	365.431	4.250	5.000	16.937	2.322	-3.894	67.392	2	73.268	-1.796	0.041	119.683	58.597	0
PV-000817165047	348.447	3.000	5.000	12.170	3.465	-3.862	285.062	3	91.174	-0.443	0.432	74.136	140.956	0
Z2923423811	339.393	3.000	6.700	14.844	1.493	-3.830	141.444	3	74.177	-1.624	-0.327	104.806	76.421	0
Z2770976320	368.333	2.000	6.250	11.894	2.457	-4.840	314.070	3	86.023	-0.736	0.033	93.801	899.591	0
Z2903058602	355.300	1.000	5.500	11.104	3.234	-5.040	789.469	3	100.000	-0.415	0.261	84.154	966.967	0
Z2218766564	359.372	2.000	5.900	10.985	2.486	-2.339	282.022	3	85.356	0.013	0.098	55.564	307.133	0
Z2193901479	325.301	1.000	6.250	10.851	2.255	-4.328	311.617	3	84.781	-1.043	-0.027	93.794	253.821	0
Z3188961853	351.450	2.000	5.000	11.613	2.714	-2.111	313.274	3	87.511	-0.028	0.105	64.688	249.539	0
PV-001862316134	351.401	3.000	4.700	12.156	3.515	-4.812	377.819	3	93.655	-1.429	0.321	96.660	172.760	0
Z2903057141	309.281	1.000	6.750	11.834	1.714	-3.386	674.823	3	87.618	-0.604	-0.223	94.641	323.389	0
Fluconazole	306.274	1	6.750	10.263	0.508	-2.074	891.697	3	82.726	-0.544	-0.449	75.149	1038.745	0

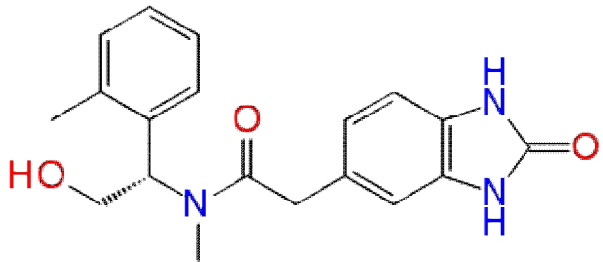
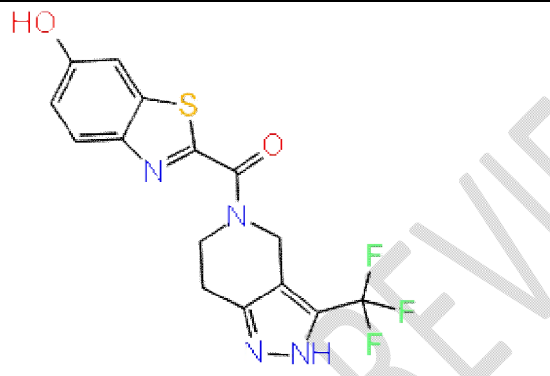
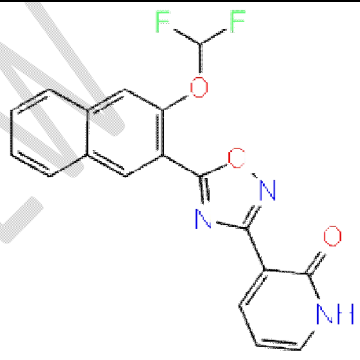
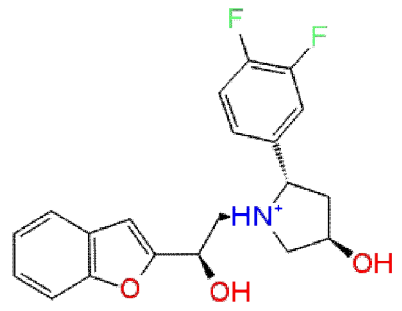
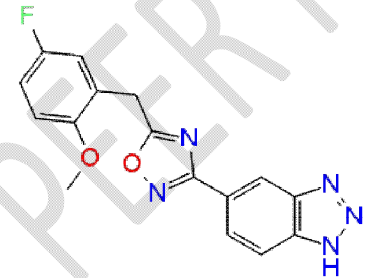
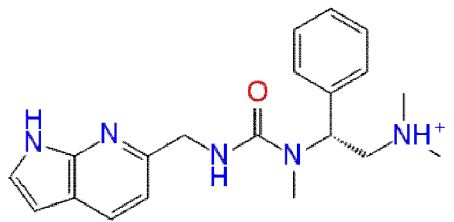
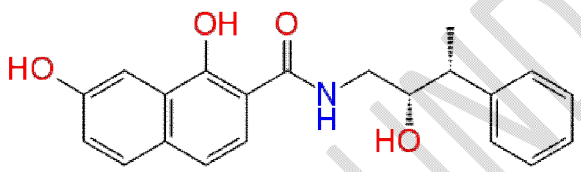
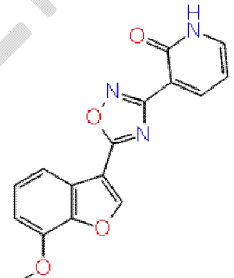
MW Molecular Weight (Acceptable range: MW < 500).; DonorHB : Estimation of the number of hydrogen bonds that the ligand can donate (Marge acceptable : 0,0 - 6,0).; AcptHB : Estimation of the number of hydrogen bonds a ligand can accept (Marge acceptable : 2,0 - 20,0).; QPlogPw: Predicted water/gas partition coefficient (Marge acceptable: 4,0 - 45 ,0).; QPlogPO/w: Predicted octanol/water partition coefficient (Marge acceptable : -2,0 – 6,5).; QPlogS: Predicted aqueous solubility, logarithm in mol dm<sup>-3</sup> (Marge acceptable : -6,5 – 0,5) ;QPPCaco: Predicted apparent Caco-2 cell permeability in nm/sec (< 25 : low et >500 : high).;PHOA : Human Oral Absorption Percentage (80% is high, and 25% is low);HOA : Predicted Oral Absorption on a scale from 1 to 3. (1: Low absorption, 2: Moderate absorption, 3: High absorption); QPlogBB (brain/blood partition coefficient) typically lies between -3.0 and 1.0; The acceptable range for QPlogKhsa (human serum albumin ;binding constant) is typically between -1.5 and 1.5.; PSA is typically less than 140 Å<sup>2</sup> for good oral bioavailability. The typical acceptable range for QPPMDCK (predicted apparent permeability in MDCK cells, measured in nm/s) is between 25 and 500. Permeability values under 25 nm/s indicate low permeability, while those exceeding 500 nm/s reflect high permeability.

Fig18 : 2D structures of the obtained hits.





 <p><b>Z1804044680</b></p>	 <p><b>Z2141883735</b></p>	 <p><b>PV-001924736320</b></p>
 <p><b>Z1545254023</b></p>	 <p><b>PV-001921223059</b></p>	 <p><b>PV-001925585102</b></p>
 <p><b>Z2095183789</b></p>	 <p><b>PV-002587460686</b></p>	 <p><b>PV-000817165047</b></p>

 <p><b>Z2923423811</b></p>	 <p><b>Z2770976320</b></p>	 <p><b>Z2903057141</b></p>	<p><b>Z290 3058 602</b></p>
 <p><b>Z2218766564</b></p>	 <p><b>Z2193901479</b></p>	 <p><b>Z3188961853</b></p>	
 <p><b>PV-001862316134</b></p>	 <p><b>Z2903057141</b></p>		

## Conclusion

A virtual screening procedure based on pharmacophore models derived from a set of antifungal molecules and the crystal structure of *Candida albicans* was applied to a compound library (Enamine) to identify new potential inhibitors of *Candida albicans*. Firstly, the Enamine database was filtered and processed to target only "drug-like" molecules. The selected set of molecules was then docked into the active site of *Candida albicans* (PDB ID: 1EA1) to assess and gain an in-depth understanding of their binding capability within the enzyme's active site.

Docking analysis revealed that the 26 identified hits interact with the active site residues in a manner similar to the reference inhibitor, fluconazole. These interactions include hydrogen bonds, pi-pi, pi-cation, and hydrophobic interactions. The predominant interactions are mainly observed with residues His259, Thr260, Phe78, Tyr76, and Hem460. Finally, an ADME study was performed for the 26 hits to assess their toxicity and pharmacokinetic properties. The analysis of the results shows that these molecules exhibit pharmacokinetic parameter values within the acceptable range for human use. The findings of this study may provide insights into the development of new potent inhibitors of *Candida albicans*.

Further studies will be necessary to better understand the stability of the hits over time within the active site of enzyme 1EA1 through molecular dynamics simulations. The molecules retained after this study will be proposed for organic synthesis and biological testing.

## Disclaimer (Artificial intelligence)

Option 2:

Author(s) hereby declare that generative AI technologies such as Large Language Models, etc. have been used during the writing or editing of manuscripts. This explanation will include the name, version, model, and source of the generative AI technology and as well as all input prompts provided to the generative AI technology

## References

1. Di Santo R (2010) Natural products as antifungal agents against clinically relevant pathogens. *Nat Prod Rep* 27:1084–1098. <https://doi.org/10.1039/b914961a>
2. Bongomin F, Gago S, Oladele RO et al. (2017) Global and Multi-National Prevalence of Fungal Diseases-Estimate Precision. *J Fungi (Basel)* 3. <https://doi.org/10.3390/jof3040057>
3. Denning DW (2024) Global incidence and mortality of severe fungal disease. *Lancet Infect Dis* 24:e428-e438. [https://doi.org/10.1016/S1473-3099\(23\)00692-8](https://doi.org/10.1016/S1473-3099(23)00692-8)
4. Vázquez-González D, Perusquía-Ortiz AM, Hundediker M et al. (2013) Opportunistic yeast infections: candidiasis, cryptococcosis, trichosporonosis and geotrichosis. *J Dtsch Dermatol Ges* 11:381-93; quiz 394. <https://doi.org/10.1111/ddg.12097>
5. Wächtler B, Citiulo F, Jablonowski N et al. (2012) *Candida albicans*-epithelial interactions: dissecting the roles of active penetration, induced endocytosis and host factors on the infection process. *PLoS ONE* 7:e36952. <https://doi.org/10.1371/journal.pone.0036952>
6. Schiaffella F, Macchiarulo A, Milanese L et al. (2005) Design, synthesis, and microbiological evaluation of new *Candida albicans* CYP51 inhibitors. *Journal of medicinal chemistry* 48:7658–7666. <https://doi.org/10.1021/jm050685j>
7. Sheehan DJ, Hitchcock CA, Sibley CM (1999) Current and Emerging Azole Antifungal Agents. *Clin Microbiol Rev* 12:40–79
8. Chimenti F, Bizzarri B, Maccioni E et al. (2007) Synthesis and in vitro activity of 2-thiazolylhydrazones compared with the activity of clotrimazole against clinical isolates of *Candida* spp. *Bioorganic & Medicinal Chemistry Letters* 17:4635–4640. <https://doi.org/10.1016/j.bmcl.2007.05.078>
9. Podust LM, Poulos TL, Waterman MR (2001) Crystal structure of cytochrome P450 14 $\alpha$ -sterol demethylase (CYP51) from *Mycobacterium tuberculosis* in complex with azole inhibitors. *Proc Natl Acad Sci U S A* 98:3068–3073. <https://doi.org/10.1073/pnas.061562898>
10. Sagatova AA, Keniya MV, Wilson RK et al. (2015) Structural Insights into Binding of the Antifungal Drug Fluconazole to *Saccharomyces cerevisiae* Lanosterol 14 $\alpha$ -Demethylase. *Antimicrob Agents Chemother* 59:4982–4989. <https://doi.org/10.1128/AAC.00925-15>
11. Luca L de (2006) Naturally occurring and synthetic imidazoles: their chemistry and their biological activities. *Curr Med Chem* 13:1–23
12. Roberts TR, Hutson DH, Lee PW et al. (2007) *Metabolic Pathways of Agrochemicals*. Royal Society of Chemistry, Cambridge
13. Zhu J, Lu J, Zhou Y et al. (2006) Design, synthesis, and antifungal activities in vitro of novel tetrahydroisoquinoline compounds based on the structure of lanosterol 14 $\alpha$ -demethylase (CYP51) of fungi. *Bioorganic & Medicinal Chemistry Letters* 16:5285–5289. <https://doi.org/10.1016/j.bmcl.2006.08.001>
14. D. Zon, A. Kone, M. Ouattara Synthèse et Activités Antifongiques de Nouveaux Benzimidazoles à Fonction 2-Arylacrylonitrile Ou 2- Cyanoarylpropénone. *Rev Ivo Ir Ci Technol* 2014 3:41–53

15. Drissa Sissouma, Mahama. Ouattara, Doumade Zon (2015) Synthesis and Antifungal Activities of Some Benzimidazolyl-Chalcones, Analogues of Chlorimidazole. *Afr. J. Pharm. Pharmacol.* 9 (12):418–423
16. Schrödinger Release 2017-4: LigPrep, Schrödinger, LLC, New York, NY, 2017.
17. Shivakumar D, Williams J, Wu Y et al. (2010) Prediction of absolute solvation free energies using molecular dynamics free energy perturbation and the OPLS force field. *Journal of chemical theory and computation* 6:1509–1519
18. Dixon SL, Smondyrev AM, Knoll EH et al. (2006) PHASE: A new engine for pharmacophore perception, 3D QSAR model development, and 3D database screening: 1. Methodology and preliminary results. *Journal of computer-aided molecular design* 20:647–671
19. Dixon SL, Smondyrev AM, Rao SN (2006) PHASE: A novel approach to pharmacophore modeling and 3D database searching. *Chemical biology & drug design* 67:370–372
20. Huang N, Shoichet BK, Irwin JJ (2006) Benchmarking sets for molecular docking. *Journal of medicinal chemistry* 49:6789–6801
21. Mysinger MM, Carchia M, Irwin JJ et al. (2012) Directory of useful decoys, enhanced (DUD-E): Better ligands and decoys for better benchmarking. *Journal of medicinal chemistry* 55:6582–6594
22. Schrödinger Release 2017-4: Phase, Schrödinger, LLC, New York, NY, 2017.
23. Braga RC, Andrade CH (2013) Assessing the performance of 3D pharmacophore models in virtual screening: How good are they? *Current topics in medicinal chemistry* 13:1127–1138
24. Yang J-M, Shen T-W (2005) A pharmacophore-based evolutionary approach for screening selective estrogen receptor modulators. *Proteins* 59:205–220. <https://doi.org/10.1002/prot.20387>
25. Clyde A, Galanie S, Kneller DW et al. (2022) High-Throughput Virtual Screening and Validation of a SARS-CoV-2 Main Protease Noncovalent Inhibitor. *J Chem Inf Model* 62:116–128. <https://doi.org/10.1021/acs.jcim.1c00851>
26. Lokwani DK, Sarkate AP, Karnik KS et al. (2020) Structure-Based Site of Metabolism (SOM) Prediction of Ligand for CYP3A4 Enzyme: Comparison of Glide XP and Induced Fit Docking (IFD). *Molecules* 25:1622. <https://doi.org/10.3390/molecules25071622>
27. Dong L, Qu X, Zhao Y et al. (2021) Prediction of Binding Free Energy of Protein-Ligand Complexes with a Hybrid Molecular Mechanics/Generalized Born Surface Area and Machine Learning Method. *ACS Omega* 6:32938–32947. <https://doi.org/10.1021/acsomega.1c04996>
28. Podust LM, Poulos TL, Waterman MR (2001) Crystal structure of cytochrome P450 14alpha -sterol demethylase (CYP51) from *Mycobacterium tuberculosis* in complex with azole inhibitors. *Proc Natl Acad Sci U S A* 98:3068–3073. <https://doi.org/10.1073/pnas.061562898>
29. Aouatef Bellamine, Galina I. Lepesheva, Michael R. Waterman (2004) Fluconazole binding and sterol demethylation in three CYP51 isoforms indicate differences in active site topology. *Journal of Lipid Research* 45:2000–2007. <https://doi.org/10.1194/jlr.M400239-JLR200>
30. Miller EB, Murphy RB, Sindhikara D et al. (2021) Reliable and Accurate Solution to the Induced Fit Docking Problem for Protein-Ligand Binding. *Journal of*

chemical theory and computation 17:2630–2639.  
<https://doi.org/10.1021/acs.jctc.1c00136>

31. Wang H, Aslanian R, Madison VS (2008) Induced-fit docking of mometasone furoate and further evidence for glucocorticoid receptor 17 $\alpha$  pocket flexibility. *Journal of Molecular Graphics and Modelling* 27:512–521
32. Saubern S, Guha R, Baell JB (2011) KNIME workflow to assess PAINS filters in SMARTS format. Comparison of RDKit and Indigo cheminformatics libraries. *Molecular Informatics* 30:847–850
33. Schrödinger Release 2017-4. Schrödinger Release 2017-4: QikProp, Schrödinger, LLC, New York, NY, 2017.
34. Dixon SL, Smondyrev AM, Knoll EH et al. (2006) PHASE: a new engine for pharmacophore perception, 3D QSAR model development, and 3D database screening: 1. Methodology and preliminary results. *Journal of computer-aided molecular design* 20:647–671. <https://doi.org/10.1007/s10822-006-9087-6>
35. Truchon J-F, Bayly CI (2007) Evaluating virtual screening methods: good and bad metrics for the "early recognition" problem. *J Chem Inf Model* 47:488–508. <https://doi.org/10.1021/ci600426e>
36. Patel S, Modi P, Chhabria M (2018) Rational approach to identify newer caspase-1 inhibitors using pharmacophore based virtual screening, docking and molecular dynamic simulation studies. *Journal of Molecular Graphics and Modelling* 81:106–115. <https://doi.org/10.1016/j.jmgs.2018.02.017>
37. Jorgensen WL, Duffy EM (2002) Prediction of drug solubility from structure. *Adv Drug Deliv Rev* 54:355–366. [https://doi.org/10.1016/s0169-409x\(02\)00008-x](https://doi.org/10.1016/s0169-409x(02)00008-x)
38. Lipinski CA, Lombardo F, Dominy BW et al. (2001) Experimental and computational approaches to estimate solubility and permeability in drug discovery and development settings. *Adv Drug Deliv Rev* 46:3–26. [https://doi.org/10.1016/s0169-409x\(00\)00129-0](https://doi.org/10.1016/s0169-409x(00)00129-0)